



Published in final edited form as:

Nature. 2015 May 7; 521(7550): 99–104. doi:10.1038/nature14424.

Allogeneic IgG combined with dendritic cell stimuli induces anti-tumor T cell immunity

Yaron Carmi¹, Matthew H. Spitzer^{1,2}, Ian L. Linde¹, Bryan M Burt³, Tyler R. Prestwood¹, Nikola Perlman¹, Matthew G. Davidson¹, Justin A. Kenkel¹, Ehud Segal¹, Ganesh V. Pusapati⁴, Nupur Bhattacharya¹, and Edgar G. Engleman¹

¹School of Medicine, Department of Pathology, Stanford University, Palo Alto, California, USA

²School of Medicine, Baxter Laboratory in Stem Cell Biology, Department of Microbiology and Immunology, Stanford University, Palo Alto, California, USA

³School of Medicine, Department of Cardiothoracic Surgery, Stanford University, Palo Alto, California, USA

⁴School of Medicine, Department of Biochemistry, Stanford University, Palo Alto, California, USA

Abstract

While cancers grow in their hosts and evade host immunity through immunoediting and immunosuppression^{1–5}, tumors are rarely transmissible between individuals. Much like transplanted allogeneic organs, allogeneic tumors are reliably rejected by host T cells, even when the tumor and host share the same major histocompatibility complex (MHC) alleles, the most potent determinants of transplant rejection^{6–10}. How such tumor-eradicating immunity is initiated remains unknown, though elucidating this process could provide a roadmap for inducing similar responses against naturally arising tumors. We found that allogeneic tumor rejection is initiated by naturally occurring tumor-binding IgG antibodies, which enable dendritic cells (DC) to internalize tumor antigens and subsequently activate tumor-reactive T cells. We exploited this mechanism to successfully treat autologous and autochthonous tumors. Either systemic administration of DC loaded with allogeneic IgG (alloIgG)-coated tumor cells or intratumoral injection of alloIgG in combination with DC stimuli induced potent T cell mediated anti-tumor immune responses, resulting in tumor eradication in mouse models of melanoma, pancreas, lung and breast cancer. Moreover, this strategy led to eradication of distant tumors and metastases, as well as the injected primary tumors. To assess the clinical relevance of these findings, we studied antibodies and cells from patients with lung cancer. T cells from these patients responded vigorously to autologous

Users may view, print, copy, and download text and data-mine the content in such documents, for the purposes of academic research, subject always to the full Conditions of use:http://www.nature.com/authors/editorial_policies/license.html#terms

Corresponding authors: Edgar G. Engleman and Yaron Carmi, ; Email: edengleman@stanford.edu and ; Email: ycarmi76@stanford.edu, Phone number: (650) 723-7960, Fax Number: (650) 725-0592

Author Contributions

Y.C. conceived the study, performed experiments and wrote the manuscript. M.H.S., I.L.L., T.R.P. and N.B. performed experiments, helped with experimental design and contributed to manuscript preparation. B.M.B. helped with experimental design, human tissue acquisition and manuscript preparation. N.P., M.G.D., J.A.K., E.S., and G.V.P. performed experiments. E.G.E. supervised the project, analyzed data, and wrote the manuscript.

Competing Financial Interests

The authors declare no competing financial interests.

tumor antigens after culture with alloIgG-loaded DC, recapitulating our findings in mice. These results reveal that tumor-binding alloIgG can induce powerful anti-tumor immunity that can be exploited for cancer immunotherapy.

To study the basis of allogeneic tumor rejection, we examined the immune response to tumors in MHC-matched allogeneic mice (illustrated in Fig. 1a). B16 melanoma cells expanded continuously in syngeneic C57Bl/6 hosts yet spontaneously regressed in allogeneic 129S1 hosts (Fig. 1b). Conversely, LMP pancreatic tumor cells, isolated from $Kras^{G12D/+};LSL-Trp53^{R172H/+};Pdx-1-Cre$ mice¹¹, grew steadily in 129S1 mice but spontaneously regressed in C57Bl/6 animals (Fig. 1b). Depletion of NK cells did not prevent tumor rejection (Extended Data 1a). In contrast, depletion of CD4⁺ or CD8⁺ T cells prior to allogeneic tumor inoculation prevented tumor regression (Fig. 1b). T cell proliferation and tumor infiltration began by week 1 (Fig. 1c, Extended Data 1b). Additionally, allogeneic tumors contained more mature myeloid DC (mDC, Ly6C⁻/CD11b⁺/CD11c⁺/MHCII⁺/CD64^{dim}) and fewer SSC^{low}/CD11b^{hi}/Ly6C^{hi}/MHCII⁻ myeloid cells than syngeneic tumors (Fig. 1d, Extended Data 1c). Even at day 3, mDC in allogeneic tumors expressed higher levels of MHCII, CD86 and CD40 compared to mDC in syngeneic tumors, reflecting activation (Extended Data 1d). Allogeneic mDC internalized more tumor cell-derived molecules from CFSE-labeled LMP cells (Fig. 1e). However, co-culture of DC with allogeneic tumor cells induced negligible activation or tumor antigen uptake (Fig. 1f, Extended Data 1e), demonstrating that additional factors contribute to DC activation *in vivo*.

Interestingly, IgM and IgG antibodies were bound to allogeneic, but not syngeneic, tumor cells within 24 hours following tumor inoculation (Fig. 1g–i), before T cells appeared (Fig. 1c). Moreover, allogeneic antibodies bound tumor cells more effectively than syngeneic antibodies (Extended Data 2a), including syngeneic antibodies from tumor-bearing mice (Extended Data 2b). To assess the potential role of antibodies in tumor rejection, B cells were depleted before mice were challenged with allogeneic tumors (Extended Data 2c). Antibody depletion accelerated tumor development and delayed or prevented tumor rejection (Fig. 1j). Moreover, adoptive transfer of allogeneic IgG, but not IgM, enabled rejection of syngeneic tumors (Fig. 1k, Extended Data 2d). This effect was abrogated in Fcγ receptor (FcγR)-deficient mice (Fig. 1k).

To investigate the effect of antibodies on tumor uptake by DC, we incubated tumor cells or lysates with syngeneic or allogeneic antibodies to form immune complexes (IC) and added these to bone marrow-derived (BM) DC (Fig. 2a). Only IC from allogeneic IgG (alloIgG-IC) or IgM (alloIgM-IC) induced BMDC activation and uptake of tumor-derived proteins (Fig. 2b–d), which were found in proximity to MHCII molecules (Fig. 2e). BMDC activated by alloIgG-IC induced significant T cell proliferation (Fig. 2f), demonstrating that tumor antigens were processed and presented.

To determine whether IC-bound DC could elicit anti-tumor immune responses in syngeneic hosts, B16 or LMP cells were inoculated subcutaneously (s.c.), and tumors were removed upon reaching 25–55mm², leaving tumor-free margins. IgG-IC or IgM-IC were prepared from excised tumors and incubated with syngeneic BMDC, which were injected into the corresponding tumor-resected mouse (Fig. 2g). While nearly all mice treated with syngeneic

BMDC loaded with alloIgG-IC remained tumor-free for over a year, all other animals experienced rapid tumor relapse (Fig. 2h). This response was completely abrogated in DC lacking Fc γ R (Extended Data 3a–c). Furthermore, adoptive transfer of T cells from alloIgG-IC-treated animals protected naïve mice from tumor challenge (Extended Data 3d–e).

Despite these findings, only minor effects were observed when alloIgG was injected into tumors in autologous hosts (Fig. 3a). To address this discrepancy, we obtained tumor-associated DC (TADC) (Extended Data 4a) and cultured them with tumor lysates or alloIgG-IC. In contrast to BMDC, TADC displayed no activation (Fig. 3b–d, Extended Data 4b) and their transfer to tumor-resected mice had no effect on recurrence (Fig. 3e). Accordingly, p38, ERK1/2 and JNK were phosphorylated in BMDC but not TADC activated with alloIgG-IC (Fig. 3f). We then tested the effect of additional MAPK stimuli on the response of TADC to alloIgG-IC. PolyI:C, TNF α +CD40L or IFN γ +CD40L enabled activation of TADC and alloIgG-IC uptake (Fig. 3g, Extended Data 4c–d). We subsequently tested whether alloIgG in combination with one of these stimuli could induce immune responses to syngeneic tumors *in situ*. Intratumoral injection of alloIgG combined with TNF α +CD40L or polyI:C induced complete elimination of B16 and LL/2 tumors (Fig. 4a, Extended Data 5a–c).

Under these conditions, only mDC (CD11b⁺/Ly6C⁻/CD11c⁺/MHCII⁺/CD64^{dim}) and cDC (CD11b⁻/CD11c^{hi}/MHCII⁺) markedly increased their IgG binding during an effective anti-tumor immune response (Fig. 4b, Extended Data 5d). Moreover, tumor-infiltrating DC exhibited significant activation (Fig. 4c) and accumulation in the draining lymph nodes (Extended Data 5e). Adoptive transfer of TADC from treated mice into naïve mice conferred complete protection against B16 (Fig. 4d). In contrast, transfer of macrophages had a modest protective effect, while B cells, NK cells and mast cells provided no benefit (Extended Data 5f–g).

To test whether alloIgG bears unique modifications that mediate an immune response, we covalently crosslinked syngeneic IgG (synIgG) onto B16 membrane proteins. These IC still conferred a therapeutic benefit after incubation with BMDC (Extended Data 6a), demonstrating that binding of IgG to the tumor cell surface, rather than the origin of the IgG, was critical. To investigate whether the tumor-binding antibody targets are related to the anti-tumor T cell specificities, we resected B16 tumor cells and formed IC using an antibody against MHC-I, against which there could not be reactive T cells. DC loaded with these IC protected animals from B16 recurrence without inducing autoimmunity, suggesting that tumor-reactive T cell specificity is not determined by the antibody targets (Extended Data 6b). Furthermore, B16-bearing mice treated with alloIgG+ α CD40+TNF α were protected from re-challenge with B16 melanoma, but not syngeneic RMA lymphoma, suggesting that the tumor-reactive T cells recognize tumor-associated antigens rather than widely expressed allo-antigens (Extended Data 6c).

Vaccination with BMDC loaded with IC containing B16 proteins derived from the cell membrane, but not other subcellular fractions, prevented tumor relapse, and B16 protein denaturation, but not deglycosylation, removed the therapeutic benefit (Extended Data 6d). Pre-absorbing alloIgG against normal cells syngeneic to the tumor also removed the therapeutic benefit (Extended Data 6e). AlloIgG from germ-free mice induced tumor

immunity (Extended Data 6f), suggesting that IgG against microbiota were not required. Therefore, the protective effect of alloIgG is dependent upon antibody binding to membrane proteins expressed on normal cells.

We therefore identified B16 membrane proteins specifically bound by alloIgG using mass spectrometry. While synIgG bound six cell membrane proteins, all at approximately equal or lower levels than alloIgG, alloIgG preferentially bound 16 cell membrane proteins, many containing strain-specific polymorphisms (Extended Data Table 1). To functionally validate these hits, we focused on Transmembrane-Glycoprotein NMB (GP-NMB). Antibodies against GP-NMB bound B16 cells at much higher levels than normal cells and enabled DC activation, and alloIgG bound GP-NMB at higher levels than synIgG (Extended Data 7a–c). Treatment using anti-GP-NMB+ α CD40+TNF α induced significant Fc γ R-dependent tumor regression (Extended Data 7d–e). Treated tumors exhibited striking leukocyte infiltration, including activated effector/memory T cells, compared to untreated tumors (Extended Data 8a–b). Whereas all treatments elicited gp100-reactive CD8⁺ T cells, only alloIgG + α CD40+TNF α elicited Trp2-reactive CD8⁺ T cells (Extended Data 8c). Adoptive transfer of CD4 or CD8 T cells from these mice protected naïve mice from B16 challenge, and depletion of either CD4 or CD8 T cells prior to treatment prevented tumor regression (Extended Data 8d–e). These findings confirm that alloIgG induces T cell reactivity against tumor-associated antigens distinct from those bound by the antibodies.

We next treated a genetically-engineered melanoma model driven by *Braf*^{V600E} and loss of *Pten*¹² with alloIgG+ α CD40+TNF α . Treated mice experienced complete responses lasting over 8 weeks in the injected tumors and distant sites (Fig. 4e). To assess the effect of this combination on metastases, orthotopic 4T1 breast tumors were treated after all mice had palpable tumor-draining lymph nodes, indicative of tumor spread. Only treatment with alloIgG+ α CD40+TNF α led to almost complete resolution of metastases and primary tumors, and the few remaining micrometastases were heavily infiltrated with leukocytes (Fig. 4f–g, Extended Data 9a).

We next compared the capacity of IgG from cancer patients and healthy allogeneic donors to bind the patients' tumors. Most but not all donors had antibodies with higher tumor-binding capacity (Extended Data 9b). We tested if alloIgG+CD40L+TNF α could induce tumor uptake and maturation of human TADC from two patients with lung carcinoma. Addition of CD40L+TNF α enabled these DC to internalize alloIgG-IC and induced DC activation (Fig. 4h, Extended Data 9c–d). Moreover, BMDC from 2 patients with malignant pleural mesothelioma incubated with alloIgG-IC, but not autologous IgG-IC, exhibited activation and drove autologous CD4⁺ T cell proliferation (Fig. 4i).

The effect of naturally arising tumor-reactive antibodies on tumor progression has been a source of controversy. Some studies suggest that such antibodies promote tumor progression^{13–19}, while others report that they can stimulate anti-tumor immunity^{20–28}. Like the antibodies that develop in cancer patients, commercial immunoglobulin preparations, which likely contain tumor-binding alloantibodies, have shown limited benefit when used to treat cancer^{29,30}. Our data may provide a mechanistic explanation for these findings, as they show that while TADC are not naturally responsive to IgG-IC, addition of specific stimuli

enables them to drive tumor-eradicating immunity. Hence, the role tumor-binding antibodies play in tumor immunity depends upon the environmental context and the cell types involved.

Here we demonstrate that tumor-antigen presentation following antibody-mediated uptake by DC is sufficient to initiate protective T cell-mediated immunity against tumors. Our work suggests that this fundamental mechanism of immunological recognition and targeting, which prevents tumor transmission even between MHC-matched individuals, can be exploited as a powerful therapeutic strategy for cancer.

Methods

Mice

129S1/SvImJ mice, C57Bl/6 WT mice, Balb/c mice, and mice that develop inducible melanoma (B6.Cg-Braf^{tm1Mmcm}/Pten^{tm1Hwu}Tg (Tyr-cre/ERT2)13Bos/BosJ) were purchased from the Jackson Laboratory (Bar Harbor, Maine) and bred on-site. CD-1 outbred mice and FcγR^{-/-} (B6.129P2-FcγR1g^{tm1Ray}) mice were purchased from Taconic (Germantown, NY). 12–16 week old mice were sorted randomly into groups before assigning treatment conditions. All mice were maintained in an American Association for the Accreditation of Laboratory Animal Care-accredited animal facility. All protocols were approved by the Stanford University Institutional Animal Care and Use Committee under protocol APLAC-17466.

Cell lines

The mouse lines B16F10 (melanoma), 4T-1.1 (breast cancer), LL/2 (Lewis lung carcinoma) and RMA (lymphoma) were all purchased from the ATCC. LMP pancreas tumor cells were isolated from Kras^{G12D/+}; LSL-Trp53^{R172H/+}; Pdx-1-Cre mice as described¹¹. Cells were cultured in DMEM (Gibco, Carlsbad, CA) supplemented with 10% heat-inactivated FCS, 2 mM L-glutamine, 100 U/mL penicillin and 100 μg/mL streptomycin (Gibco) under standard conditions.

Preparation and in vitro studies of mouse DC subsets

BM mononuclear cells were negatively selected using a murine monocyte enrichment kit (Stem Cell Technologies, Vancouver Canada), and FSC^{lo}/SSC^{lo}/Ly6C^{hi}/CD115^{hi}/MHCII^{neg} cells were sorted with a FACS Aria II (BD Biosciences). Monocytes were cultured for 4–5 days in the presence of 50 ng/mL GM-CSF (PeproTech) to generate DC. For TADC, tumors were digested in Hank's balanced salt solution (HBSS, Gibco) containing 4 mg/mL collagenase IV and 0.01 mg/mL DNase I (Sigma). Cells were applied on a Ficoll gradient and magnetically enriched using CD11b⁺ selection kits (StemCells) and Ly6C⁻/CD11c⁺/MHCII⁺ cells were sorted by FACS. In some experiments TADC were activated with 1 μg/mL bacterial lipopolysaccharide (LPS), 1 μg/mL high molecular weight polyinosinic-polycytidylic acid (polyI:C) (both from InvivoGen, San Diego, CA), or with 50 ng/mL TNFα or 50 ng/mL IFNγ (PeproTech) in combination with 500 ng/mL CD40L, OX-40 (PeproTech) or 500 ng/mL CD28 (R&D) recombinant mouse proteins. All *in vitro* activations of mouse DC were independently repeated at least 10 times in duplicate.

Preparation and in vitro studies of tumor cells, TADC, autologous T cells and IgG from patients with cancer

Tumor cells, TADC, peripheral blood T cells and IgG were obtained from 2 patients undergoing resection surgery for stage I lung carcinoma. Tumors were enzymatically digested with 0.1mg/mL of DNase I and 5mg/mL collagenase IV (Sigma) in HBSS for 30 min. Tumor cells were enriched by sorting CD45-negative cells, fixed in 2% paraformaldehyde for 20 min, washed extensively in PBS and coated for 30 min with autologous IgG or pooled allogeneic IgG obtained from healthy blood donors. To obtain TADC, FSC^{low}/SSC^{low}/CD11c⁺/MHCII^{hi} cells were sorted and maintained for 1h in 10% FCS IMDM at 37°C. For FACS and confocal studies, tumor DC were incubated overnight with autologous tumor cells coated with selfIgG or alloIgG alone, or in the presence of 5 ng/mL recombinant human TNF α and 500 ng/mL CD40L (PeproTech).

In separate experiments, 10 cm long rib bones and 10 mL blood were obtained from 2 patients undergoing resection surgery for malignant pleural mesothelioma. To generate BMDC, bones were flushed with PBS and mononuclear cells were separated on Ficoll gradients. CD34⁺ cells were then enriched using magnetic beads (Miltenyi) and cultured for 9–12 days in IMDM (Gibco) supplemented with 10% FCS, 50 ng/mL human GM-CSF and 20 ng/mL human IL-4 (PeproTech). To obtain autologous tumor cells, tumors were enzymatically digested with 0.1mg/mL of DNase I and 5mg/mL collagenase IV (Sigma) in HBSS for 30 min. Tumor cells were enriched by sorting CD45-negative cells, fixed in 2% paraformaldehyde for 20 min, washed extensively in PBS and coated for 30 min with autologous or pooled allogeneic IgG. Autologous CD4⁺ T cells were enriched from peripheral blood mononuclear cells on magnetic beads (Miltenyi) and IgG was isolated from each patient's plasma using protein A columns (GE Healthcare). For T cell proliferation assays, 2×10^4 DC were incubated overnight with antibody-coated tumor cells as above, washed and co-cultured with 2×10^5 autologous CD4⁺-enriched T cells. After 6 days, cells were pulsed with ³H-thymidine (1 μ Ci/well) and cultured for an additional 18h before being harvested in a Harvester 400 (Tomtec). Radioactivity was measured by a 1450 MicroBeta counter (LKB Wallac). T cell proliferation was assayed in 6 technical replicates per sample. The human subjects protocols were approved by Stanford's Institutional Review Board, and informed consent was obtained from all subjects.

Flow cytometry

For cell surface staining, monoclonal antibodies conjugated to FITC, PE, PE-Cy7, PE-Cy5.5, APC-Cy7, eFluor 650, or Pacific Blue and specific for the following antigens were used: CD11b (M1/70), F4/80 (BM8), B220 (RA3-6B2) from BioLegend (San Diego, CA) and CD115 (AFS98), CD80 (16-10A1), I-Ab (AF6-120.1), CD40 (1C10), Ly6C (HK1.4), CD86 (GL1) from eBioscience (San Diego, CA). All *in vivo* experiments to characterize tumor-infiltrating leukocytes were independently repeated at least 3 times with 3–5 mice per group. iTA α APC-labeled H-2K^b-Trp-2 (SVYDFVWL) and iTA α PE-labeled H-2D^b-gp100 (EGSRNQDWL) tetramers were purchased from MBL international (Woburn, MA) and were used according to manufacturer's instructions. Tetramer-staining experiments were repeated twice with 5 mice in each group. For protein phosphorylation-specific flow cytometry, cells were activated for 5, 15 or 30 min with or without IC and fixed for 15 min

with 1.8% paraformaldehyde. Cells were washed twice with PBS containing 2% FCS and incubated with 95% methanol at 4°C for 20 min. Conjugated antibodies against phospho-p38 (Thr180/Tyr182), and phospho-JNK (Thr183/Tyr185) were purchased from Cell Signaling and phospho-ERK1/2 (p44) (pT202/pY204) from BD Biosciences. DC protein phosphorylation experiments were repeated 5 times, each with biological duplicates. For tumor-binding IgM and IgG, PE-conjugated anti-mouse IgM (RMM-1), anti-mouse IgG (Poli4052) and anti-human IgG (HP6017) were purchased from BioLegend. Flow cytometry was performed on a LSRII (BD Biosciences) and datasets were analyzed using FlowJo software (Tree Star, Inc.). *In vivo* binding levels were tested in 4 independent experiments, 3–5 mice in each group.

Intracellular IFN γ staining

B16 tumors from treated mice were digested to obtain a single cell suspension. A total of 2×10^6 cells per well were cultured for 4 hours in 10% FCS RPMI containing $1 \times$ Brefeldin A (eBioscience) in a 96 well plate containing 4×10^4 BMDC loaded with 10 μ g of B16 membrane proteins. Cells were washed and stained for extracellular T cell markers. Cells were then fixed and permeabilized using cytofix/cytoperm solutions (BD Bioscience) and stained with PE-Cy7 conjugated anti-IFN γ antibody (XMG1.2, BioLegend). Experiments were repeated twice independently with 5 mice per group.

Cytokine measurements

Cells were seeded at 1×10^6 cells/mL and cultured for 12 h with or without tumor immune complexes, or LPS (Sigma). TNF α , IFN γ , and IL-12 (p40/p70) in the supernatants were measured by ELISA, according to manufacturer's instructions (R&D Systems, Minneapolis, MN). Cytokine secretion was measured in biological triplicates in 4 independent experiments.

IgG and IgM purification and measurement

Mouse antibodies were obtained from pooled 5 mL 20–24-week-old mouse serum by liquid chromatography on AKTA Explorer/100Air (GE Healthcare). Total mouse IgG and IgM were purified using protein-G and 2-mercaptopyridine columns, respectively (GE Healthcare). The levels of purified IgG and IgM were measured with specific ELISA kits (Bethyl, Montgomery, TX) according to manufacturer's instructions. The capacity of purified antibodies to bind tumor cells was tested by flow cytometry prior to their use *in vivo*. 1 μ g IgG per 1×10^5 allogeneic tumor cells bound at least 8 times higher compared to isotype control antibodies. Serum levels of antibodies were measured in biological triplicates in 4 independent experiments.

Necrotic and apoptotic tumor cell internalization experiments

For necrotic tumor cells, cultured LMP or B16 cell were trypsinized, washed and resuspended at a concentration of 5×10^6 cells/mL in cold PBS (GIBCO). Cells were then subjected to three cycles of freeze-thaw between liquid nitrogen and a 37°C water bath and the level of necrotic cells was determined by Trypan blue under light microscopy. Apoptotic tumor cells were prepared by their pre-incubation with 25 μ g/mL of mitomycin C (Sigma)

for 1 hour in antibiotic and serum-free DMEM. Fluorescein labeled *E. coli* BioParticles were purchased from Life Technologies and used according to the manufacturer's instructions. DC activations with above cells were repeated 4 independent times in biological duplicates.

Preparation of antibody-tumor lysate immune complexes (Ig-IC) and antibody-bound tumor cells

When obtained from surgical resections, tumor cells were initially isolated after enzymatic digestion and sorted as FSC^{hi}/CD45^{neg} cells prior to their fixation and staining. For tumor-antibody complexes, tumor cells were fixed in 2% paraformaldehyde, washed extensively and incubated with 1–3 µg syngeneic or allogeneic IgG or IgM per 1×10⁵ tumor cells, and were then washed to remove excess antibodies. To obtain tumor lysate Ig-IC, tumor cells were incubated for 30 min on ice with 1–3 µg syngeneic or allogeneic IgG or IgM per 1×10⁵ tumor cells, washed from excess antibodies and further disrupted with non-denaturing lysis buffer (Pierce) to obtain Ig-IC. DC activations with the above Ig-IC were repeated in at least 10 independent experiments in biological duplicates.

Absorption of alloIgG on normal cells

Skin and pancreas were removed from naïve C57Bl/6 or 129S1 mice and enzymatically digested with 0.1 mg/mL of DNase I (Sigma) and 4 mg/mL collagenase IV (Sigma) in PBS to obtain single cell suspensions. Splenocytes were isolated by mashing spleens through 70 µm cell strainers. Cells were then mixed at 1:1:1 ratio and extensively washed and incubated with 0.5 µg/1×10⁶ cells FcγR block (BD) and 5% (W/V) BSA (Sigma) in PBS for 15 min on ice. Cells were then washed and incubated with alloIgG (2 µg per 1×10⁶ cells) for 30 min on ice. Cells were centrifuged at 5,000 RPM for 10 min, and the supernatants were concentrated by 50 kDa centrifugal filters (Amicon) before being incubated with 1×10⁵ tumor cells.

Membrane protein extraction

For native membrane protein extraction, B16F10 cells were scraped in cold PBS and pelleted at 400×g for 5 min at 4°C. The cell pellet was washed twice in cold PBS, resuspended in 10 mM HEPES pH 7.4 and incubated on ice for 10 min. Cells were pelleted and the buffer was removed. The cell pellet was resuspended in 10 mL of SEAT buffer (10 mM triethanolamine/acetic acid, 1 mM EDTA pH 8.0, 250 mM sucrose, protease inhibitor cocktail) and homogenized with twenty strokes of a dounce homogenizer. The sample was spun at 900×g for 6 min to collect the post-nuclear supernatant (PNS). The PNS was spun at 100,000×g for 60 min at 4°C to harvest a membrane pellet, which was then resuspended in 4 mL membrane extraction buffer (MEB) containing 50 mM Tris-HCl pH-8.0, 150 mM NaCl, 1% NP-40, 1 mM DTT, 10% glycerol, 1 mM NaF, and protease inhibitor cocktail. After incubation for 2 h at 4°C, the membrane extract was clarified by centrifugation at 100,000×g for 30 min at 4°C. For denatured membrane protein extraction, the membrane pellet was resuspended in 500 µl Radio-Immuno-Precipitation Assay buffer (RIPA, Sigma) and lysed with a 25G needle syringe. Lysates were incubated at 4°C for 1h and spun at 100,000×g, 30min, 4°C. Supernatant containing detergent solubilized membrane proteins was collected and boiled for 5min at 95°C. Deglycosylation of membrane proteins was performed using a commercial kit (New England Biolabs, Ipswich, MA) according to the manufacturer's

instructions. Isolation of cell-membrane proteins was repeated 3 independent times and the running pattern of precipitated proteins was compared on SDS-PAGE.

Immunoprecipitation and mass spectrometry

Immunoprecipitation was set up with 20 mg membrane extract and 50 µg of syngeneic or allogeneic IgG coupled to protein G magnetic beads and incubated for 16 hr at 4°C. Beads were washed thrice with MEB and bound protein complexes were eluted with 2X Laemmli buffer. The eluted sample was subjected to SDS-PAGE on a 4–12% Bis-Tris gel followed by GelCode Blue staining (Thermo Scientific) to visualize protein bands. Protein bands were excised, digested with trypsin and analyzed (MS Bioworks) using a nano LC/MS/MS with a NanoAcquity HPLC system (Waters) interfaced to a Q Exactive (Thermo Fisher). The mass spectrometer was operated in data-dependent mode, with MS and MS/MS performed in the Orbitrap at 70,000 FWHM and 17,500 FWHM resolution, respectively. The fifteen most abundant ions were selected for MS/MS. The data were processed with the Mascot Server (Matrix Science). Mascot DAT files were parsed into the Scaffold software for validation, filtering and to create a non-redundant list per sample. Data were filtered at 1% protein and peptide FDR, requiring at least two unique peptides per protein. Mass spectrometry analysis of precipitated proteins was performed once.

Native gel and tumor cell GP-NMB staining

Recombinant mouse GP-NMB (R&D) was mixed with native loading buffer (16% Glycerol, 1% Trypan blue and 50 mM pH 7.0 Tris-HCl) and 62.5 and 125 ng/well was run for 2 hours in Novex® NativePAGE™ Bis-Tris gel system (Life Technologies) on ice. Bands were transferred to a nitrocellulose membrane and incubated overnight with 10µg/mL mouse IgG, or with 1µg/mL rabbit polyclonal IgG anti-mouse GP-NMB (cat. no. S-24 sc-133634, Santa Cruz). The membranes were washed, incubated for 45min with goat anti-mouse IgG light chain-specific antibodies conjugated to HRP (Pierce), developed with SuperSignal West Femto Substrate (Pierce), and exposed together for imaging.

For FACS staining of GP-NMB on tumor cells, 1×10^5 B16 or LMP cells were incubated with 2µg rabbit polyclonal anti-mouse GP-NMB (Santa Cruz) for 30 min, washed twice and incubated for 20 min with PE-conjugated donkey anti-rabbit or goat anti-mouse antibodies, respectively (both from eBioscience). FACS measurements were repeated 3 independent times in biological duplicates.

In vivo tumor models

For tumor challenge studies, 2×10^5 and 5×10^4 LMP or B16 tumor cells, respectively, were injected subcutaneously (s.c.) above the right flank, and tumor development was measured twice a week with calipers. In some experiments, $1-2 \times 10^6$ tumor cells were labeled with 25 µM CFSE according to manufacturer's instructions (Invitrogen). Tumor challenge experiments were repeated independently at least 8 times with 4 mice per group. For prophylactic immunization, mice were injected twice s.c., 7 days apart, with 2×10^6 DC or monocytes that were loaded with tumor lysates or IC. This was independently repeated 3 times with 4 mice per group. For tumor recurrence studies, 2×10^5 tumor cells were injected s.c. above the right flank, and the size of growing tumors was measured using calipers.

When tumors reached 45–55 mm² for LMP and 12–16 mm² for B16, mice were anesthetized and visible macroscopic tumor was surgically removed. Resected tumors were enzymatically digested with 0.1mg/mL of DNase I (Sigma) and 5mg/mL collagenase IV (Sigma) in HBSS. Cells were then fixed in 2% paraformaldehyde for 20 min, washed extensively in PBS and coated for 30 min with syngeneic or allogeneic antibodies. In some experiments, tumor cells were coated with mouse anti-mouse anti-H2-K^b (2µg/1x10⁵ cells) or its isotype control (C1.18.4, both from BioXcell). Antibody-coated tumor cells were then washed and added to DC cultures. After overnight incubation, DC were washed and 2.5x10⁶ were injected s.c. to tumor-resected mice one day after the tumors were removed, adjacent to the site of tumor resection. This experiment was repeated independently at least 3 times with 4 mice per group. For *in vivo* tumor treatments, a combination of 2 µg TNFα (Peprotech) and 100 µg agonistic αCD40 (FGK4.5, BioXcell), 5 µg recombinant CD40L (PeproTech), 5 µg CD28 (R&D Systems, Minneapolis, MN), 5 µg LPS or 200 µg polyI:C (Invivogen), and 400 µg mouse allogeneic or syngeneic IgG or anti-GP-NMB (Santa Cruz), was injected twice (2 days apart) directly into tumors. Experiments were repeated independently at least 5 times with 4–5 mice per group. For treatment of the Braf^{V600E} melanoma model, mice were injected twice (2 days apart) in 2 cycles, one week apart, with 1mg IgG derived from CD-1 mice along with TNFα and αCD40 once the largest tumor nodule reached 16mm². For metastasis experiments, 1x10⁵ 4T-1 cells were injected into the mammary fat pad of syngeneic Balb/c mice. After 14–16 days, once tumors metastasized into the draining lymph node, the primary tumor nodules were injected twice (2 days apart) in 2 cycles, one week apart, with 1mg IgG derived from CD-1 mice along with TNFα and αCD40. Experiments were repeated independently at least 3 times with 3–5 mice per group.

In vivo binding of PE-labeled alloIgG

Allogeneic antibodies were fluorescently labeled with PE using Lightning-Link® kits according to the manufacturer's instructions (Innova Biosciences Ltd., Cambridge, UK). Subsequently, 5 µg of labeled alloIgG was injected intratumorally alone or with TNFα and αCD40. After 2 h, tumors were enzymatically digested to obtain a single cell suspension and the PE levels were analyzed by flow cytometry along with lineage markers.

Covalent binding of syngeneic antibodies to tumor cells

Syngeneic IgG was cross-linked to primary amines of B16 cell surface proteins using sulfo-LC-SPDP (sulfosuccinimidyl 6-(3'-[2-pyridyldithio]-propionamido) hexanoate, Pierce) according to the manufacturer's instructions. Briefly, both the antibodies and cells were initially treated with sulfo-LC-SPDP to label primary amines. Next, disulfide bonds in syngeneic IgG were reduced by treatment with DTT. Finally, the reduced syngeneic IgG was incubated with SPDP-labeled B16 cells and the level of binding was later assessed by flow cytometry. Experiments were repeated independently 3 times with 4 mice per group.

In vivo cell depletion

Depletion of CD4⁺ and CD8⁺ T cells was achieved by intraperitoneal (i.p.) injection of 500 µg/mouse GK1.5 (anti-CD4) and YST-169.4 (anti-CD8) monoclonal antibodies (both from BioXcell, West Lebanon, NH), respectively, 3 days before tumor inoculation and every 3 days thereafter. T cell depletion experiments were repeated independently 3 times for each

depletion antibody with 3–4 mice per group. In some experiments, B16-bearing mice were injected with 500 µg/mouse anti-CD8 or anti-CD4 2 days prior to their treatment with antibodies+TNFα+αCD40 and once a week thereafter. These T cell depletion experiments were repeated independently 2 times for each depletion antibody with 5 mice per group. For B cell depletion, 300 µg/mouse anti-CD19 (1D3) and 300 µg/mouse anti-B220 (RA3.3A1/6.1) (both from BioXcell) were injected i.p. three weeks before tumor inoculation and every 5 days thereafter. B cell depletion experiments were repeated independently 3 times with 3–5 mice per group. For NK cell depletion, mice were injected i.p. with 50 µl anti-asialo (GM1) polyclonal antibody (Wako Chemicals, Richmond, VA), or with 200 µg anti-NK1.1 (PK136) (BioXCell) on days –2, 0, 4, and 8 relative to tumor challenge. Individual mice were bled on days 0, 7, 14 and 21 and the levels of NK1.1⁺/CD3ε^{neg} cells were determined by flow cytometry to confirm depletion. NK cell depletion experiments were repeated independently 3 times with anti-asialo depletion antibody with 3–5 mice per group.

Adoptive transfer

Mice were injected i.v. with 1 mg/mouse of syngeneic or allogeneic IgG or IgM one day prior to tumor challenge and once again with tumor injection. For T cell transfer, splenic CD4⁺ and CD8⁺ T cells were negatively selected using a murine enrichment kit (Stem Cell Technologies) and at least 5x10⁶ cells were injected i.v. to recipient mice one day before tumor challenge. T cell adoptive transfer experiments were repeated independently 3 times for each T cell subset with 3–5 mice per group. Prior to their transfer, tumor-associated cell subsets were enriched as follows: TADC were isolated by enrichment of MHCII⁺ cells on magnetic beads (Miltenyi) and subsequent sorting of Ly6C^{neg}/CD11c⁺/CD64^{dim} by FACS. Tumor macrophages were enriched with CD11b⁺ magnetic beads (Miltenyi) followed by sorting of Ly6C^{neg}/CD64^{hi} cells. B cells were enriched with CD19⁺ magnetic beads (Miltenyi). NK cells were enriched with NK1.1⁺ magnetic beads (Miltenyi), and mast cells were enriched with c-kit⁺ magnetic beads (Miltenyi). For each cell subset, 2x10⁶ cells were injected s.c. into naïve mice 3 days before being challenged with 5x10⁴ B16 tumor cells. Transfer experiments for each cell type were repeated 3 times independently with 3–5 mice per group.

T cell proliferation

3x10⁴ DC were co-cultured with 3x10⁵ MACS-enriched CD4⁺ T cells (Miltenyi, Germany) from spleens of LMP- or B16-immunized mice. After 6 days, cells were pulsed with ³H-thymidine (1 µCi/well) and cultured for an additional 18h before being harvested in a Harvester 400 (Tomtec). Radioactivity was measured by a 1450 MicroBeta counter (LKB Wallac). T cell proliferation was repeated 5 times with 3 biological replicates and 6 technical replicates for each.

In vivo BrdU incorporation

Tumor-challenged mice were injected i.p. every day with 1mg of 5-bromo-2-deoxyuridine (BrdU) in 200 µL PBS. At several time points, mice were sacrificed and single cell suspensions were prepared from BM, lymph nodes and tumor tissues. Cells were then stained for lineage markers followed by intracellular staining with FITC-conjugated anti-

BrdU antibody according to manufacturer's instructions (BD Pharmingen) and analyzed by flow cytometry. Experiments were repeated independently 3 times with 3–5 mice per group.

Immunofluorescence

DC or monocytes were incubated on glass-bottom culture plates (In Vitro Scientific) with CFSE-labeled tumor cells with or without antibodies overnight. Cells were gently washed with PBS (Gibco), fixed for 20 min with 2% paraformaldehyde and permeabilized with 0.5% saponin (Sigma). Samples were blocked with 10% non-immune goat serum and stained with Alexa-conjugated anti-mouse IgG and IgM (Invitrogen 1:100) and anti-mouse I-Ab (BD Biosciences, 1:100). DC immunostainings were independently repeated at least 3 times in biological duplicates and 3 fields were documented in each slide.

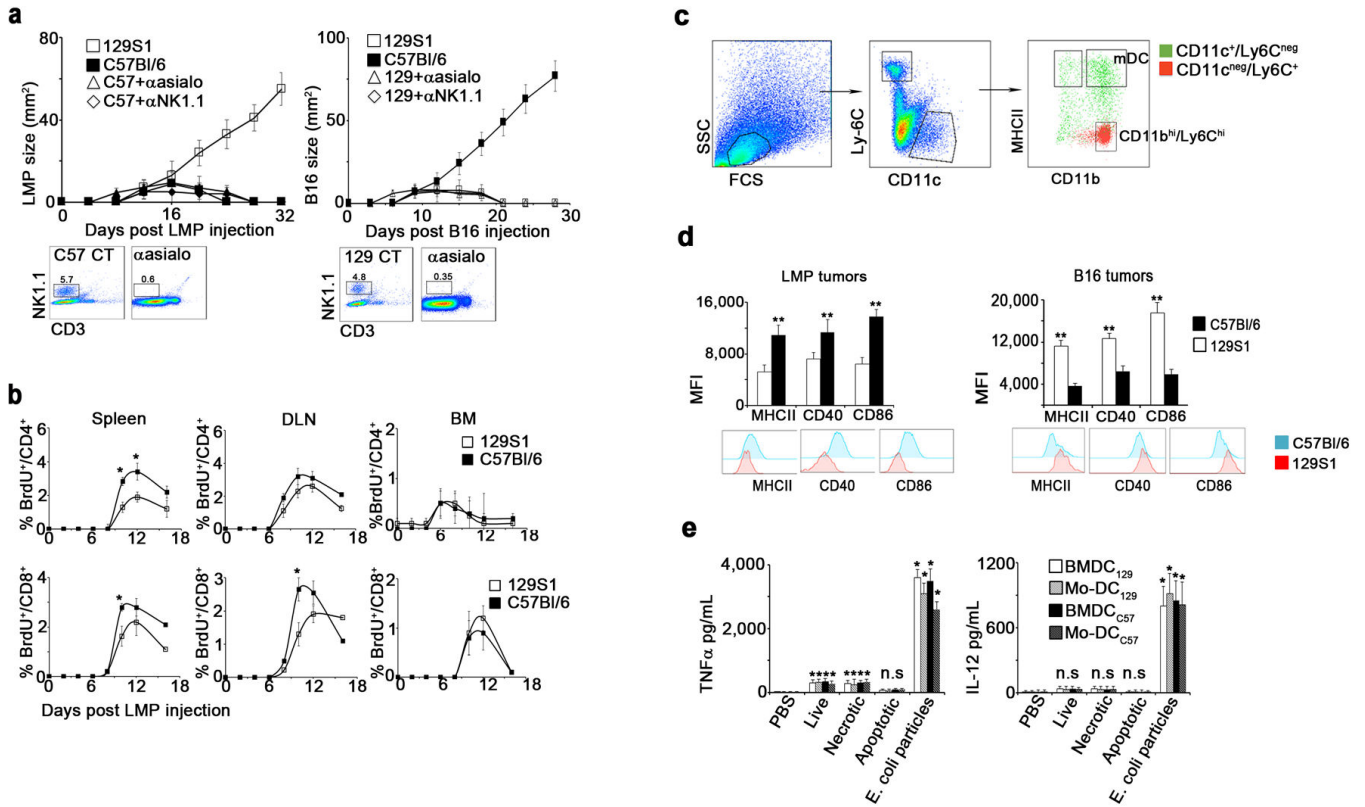
Immunohistochemistry

Specimens were fixed in 4% paraformaldehyde, equilibrated in a 20% sucrose solution and embedded in frozen tissue matrix (Tissue-Tek OCT, Torrance, CA). Slides were cut to 5 μm , blocked with 10% non-immune goat serum and stained with goat anti-mouse IgG (Invitrogen 1:100) and anti-mouse IgM (II/41 eBioscience, 1:100). Sections were examined under a Zeiss Laser Scanning Confocal Microscope. Images were collected using a Zeiss 700 confocal laser scanning microscope, and analyzed using ZEN software (Carl Zeiss Microscopy). Tumor immunostainings were repeated independently at least 3 times in biological duplicates and 3 fields were captured for each slide.

Statistics

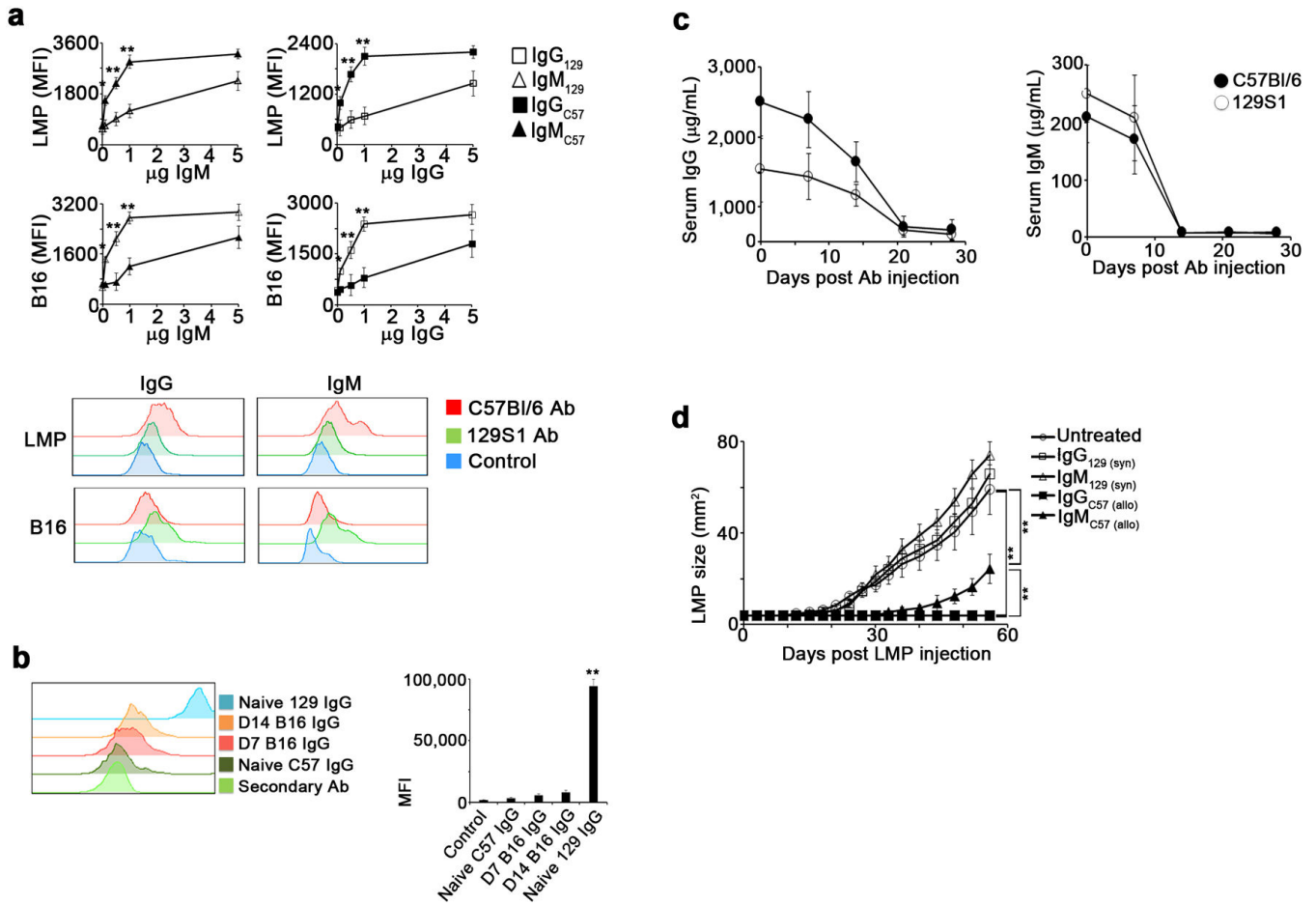
Sample size was chosen such that statistical significance could be achieved using appropriate statistical tests (e.g. ANOVA) with errors approximated from previously reported studies. A non-parametric Mann–Whitney U test was performed in Prism (GraphPad Software, Inc.) to analyze experimental data, unless otherwise stated. Phospho-specific flow cytometry data were transformed by taking the inverse hyperbolic sine (arcsinh), and ratios were taken over the corresponding baseline (unstimulated) value as previously described (Irish et al., PNAS, 2010). No blinded experiments were performed. No samples were excluded from analyses. P values indicate significance of the difference between experimental and control (CT) values. * denotes $p < 0.05$; ** denotes $p < 0.01$. Error bars represent \pm SEM.

Extended Data



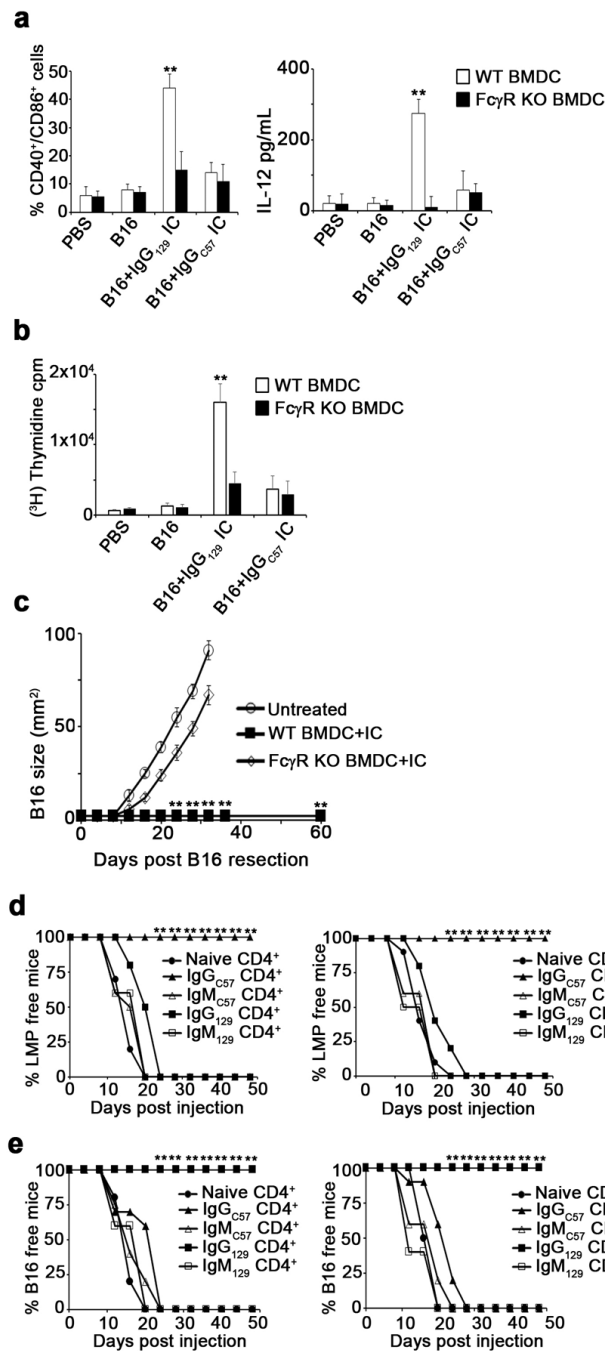
Extended Data 1.

a. LMP (left) and B16 (right) growth in 129S1 (□) C57Bl/6 (■), or allogeneic hosts pretreated with anti-asialo-GM1 (△) or anti-NK1.1 antibodies (◇) (n=6). Shown are representative plots of NK cells in the blood prior to tumor challenge. **b.** BrdU incorporation by CD4⁺ T cells (top graphs) and CD8⁺ T cells (bottom graphs) in lymphoid organs of 129S1 (□) and C57Bl/6 (■) LMP-bearing mice (n=8). **c.** Representative flow cytometric analysis of CD11b^{hi}/Ly6C^{hi} myeloid cells and mature DC (mDC) on day 10 after C57Bl/6 mice were inoculated with B16 tumor cells. **d.** Flow cytometric analysis of Ly6C^{neg}/CD11c⁺/MHCII⁺ cells from LMP-bearing mice (left panel) and B16-bearing mice (right panel). Histograms show representative expression levels of co-stimulatory molecules on DC from C57Bl/6 (■) and 129S1 mice (■) (n=8). **e.** IL-12 (right) and TNFα (left) in the supernatants of syngeneic BMDC (□), syngeneic blood monocyte-derived (Mo)-DC (▨), allogeneic BMDC (●) or Mo-DC (▩) incubated with live, frozen-thawed (necrotic), or mitomycin C-treated (apoptotic) LMP cells or *E. coli* BioParticles overnight (n=8). Shown are the mean values ±SEM from two independent experiments. Asterisk (*) denotes *p*<0.05 and two asterisks (**) denote *p*<0.01.



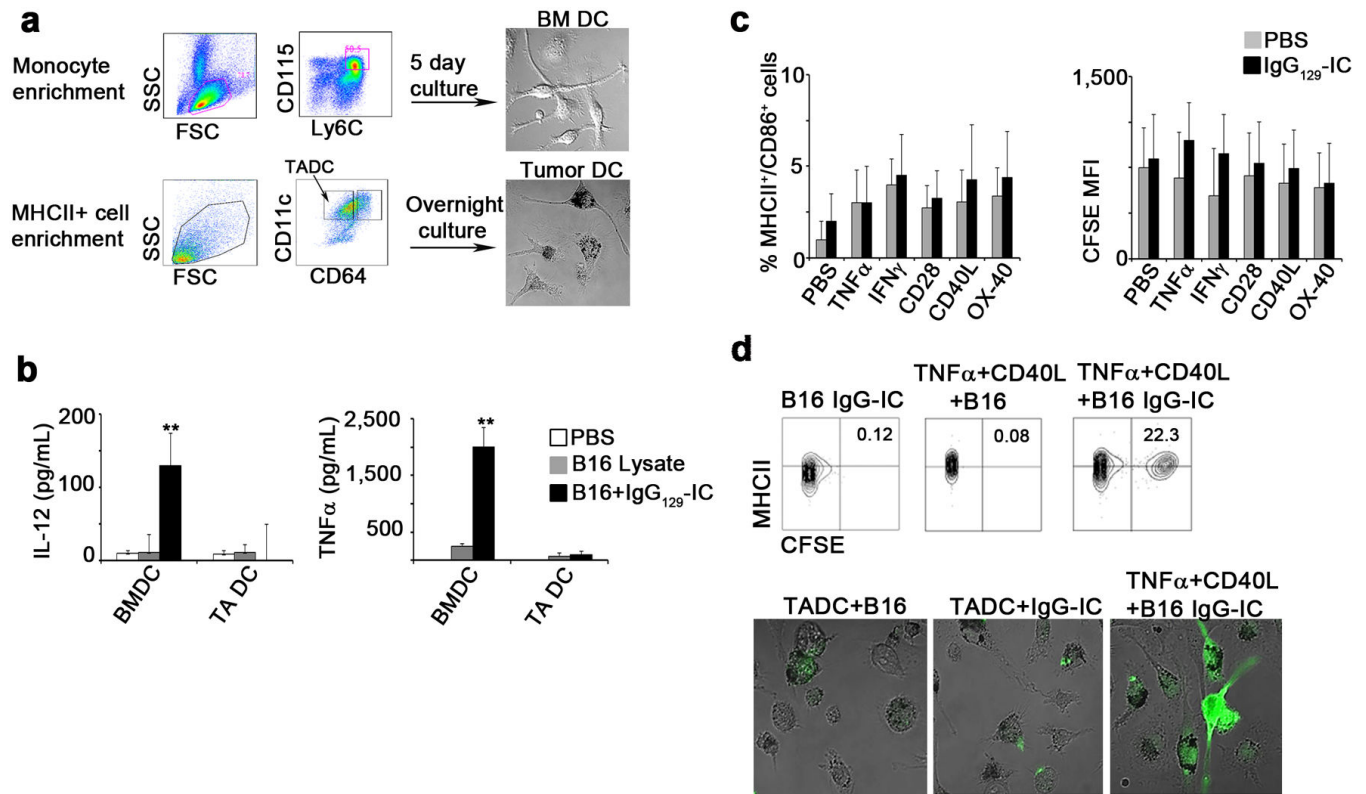
Extended Data 2.

a. Flow cytometric analysis of the binding of various concentrations of IgG from 129S1 (\square), IgM from 129S1 (\diamond), IgG from C57Bl/6 (\blacksquare) and IgM from C57Bl/6 mice (\blacktriangle) to LMP and B16 cells. The lower panel shows a representative histogram of IgG (left) or IgM (right) binding after incubation of $1\mu\text{g}$ of C57Bl/6 (\blacksquare) or 129S1 (\square) antibodies with 1×10^5 LMP (upper) or B16 (lower) cells ($n=8$). **b.** The left panel shows a representative histogram of the MFI of IgG after incubation of $2\mu\text{g}$ of either control antibody (\square) or IgG from the serum of naïve C57Bl/6 mice (\blacksquare), B16-bearing C57Bl/6 mice on day 7 (\blacksquare), B16-bearing C57Bl/6 mice on day 14 (\blacksquare) or naïve 129S1 mice (\square) with 1×10^5 B16 cells ($n=6$). Right graph shows MFI of the binding of $2\mu\text{g}$ of each IgG to 1×10^5 B16 cells. **c.** Serum levels of IgG (left) and IgM (right) in C57Bl/6 (\bullet) and 129S1 mice (\circ) following i.p injection with anti-B220 and anti-CD19 antibodies ($n=8$). **d.** LMP tumor size in naïve 129S1 mice injected with allogeneic IgG (\blacksquare), allogeneic IgM (\blacktriangle), syngeneic IgG (\square) or syngeneic IgM (\triangle) on days -1 and 0 relative to tumor injection ($n=6$). Shown are the mean values \pm SEM from two independent experiments. Asterisk (*) denotes $p < 0.05$ and two asterisks (**) denote $p < 0.01$.

**Extended Data 3.**

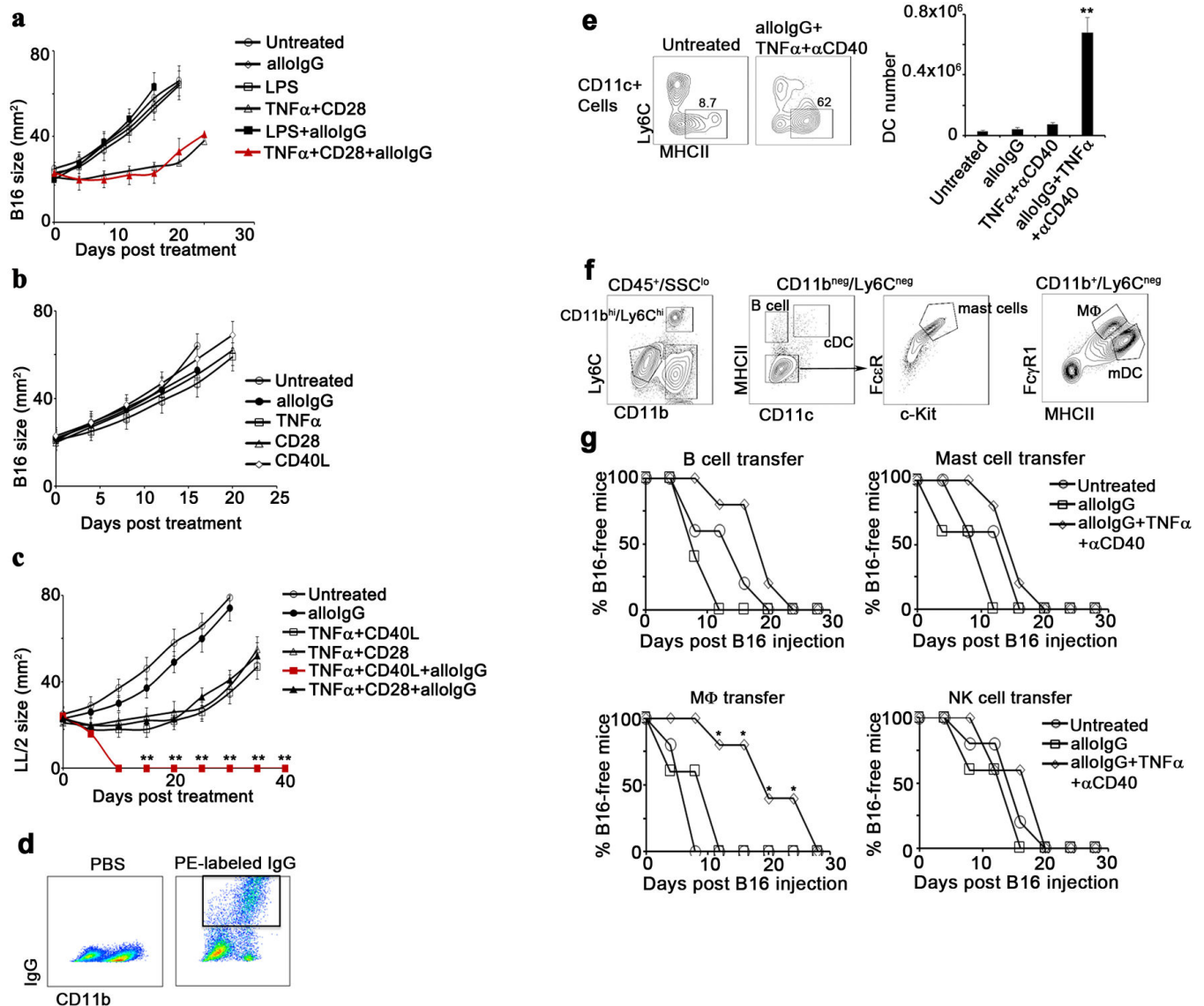
a. Mean levels of CD40 and CD86 expression (left) and IL-12 secretion (right) in BMDC from C57Bl/6 (□) and Fc γ R KO mice (■) activated with IgG-IC overnight (n=6). **b.** Proliferation of CD4⁺ T cells cultured with BMDC from C57Bl/6 (□) and Fc γ R KO mice (■) loaded with IgG-IC (n=4). **c.** Tumor recurrence in untreated mice (○), mice treated with WT BMDC loaded with IgG-IC (■), or mice treated with Fc γ R KO BMDC loaded with IgG-IC (◇) (n=8). **d. and e.** Percentages of tumor-free mice following adoptive transfer of 5×10^6 splenic CD4⁺ T cells (left graph) or CD8⁺ T cells (right graph) from naive mice (●),

or from LMP (d)- or B16 (e)-resected mice treated with DC+IgG_{C57} IC (▲), DC+IgM_{C57} IC (△), DC+IgG₁₂₉ IC (■), or DC+IgM₁₂₉ IC (□), and subsequently challenged with LMP (d) or B16 (e) (n=6). Shown are the mean values ±SEM from two independent experiments. Asterisks (**) denote p<0.01.



Extended Data 4.

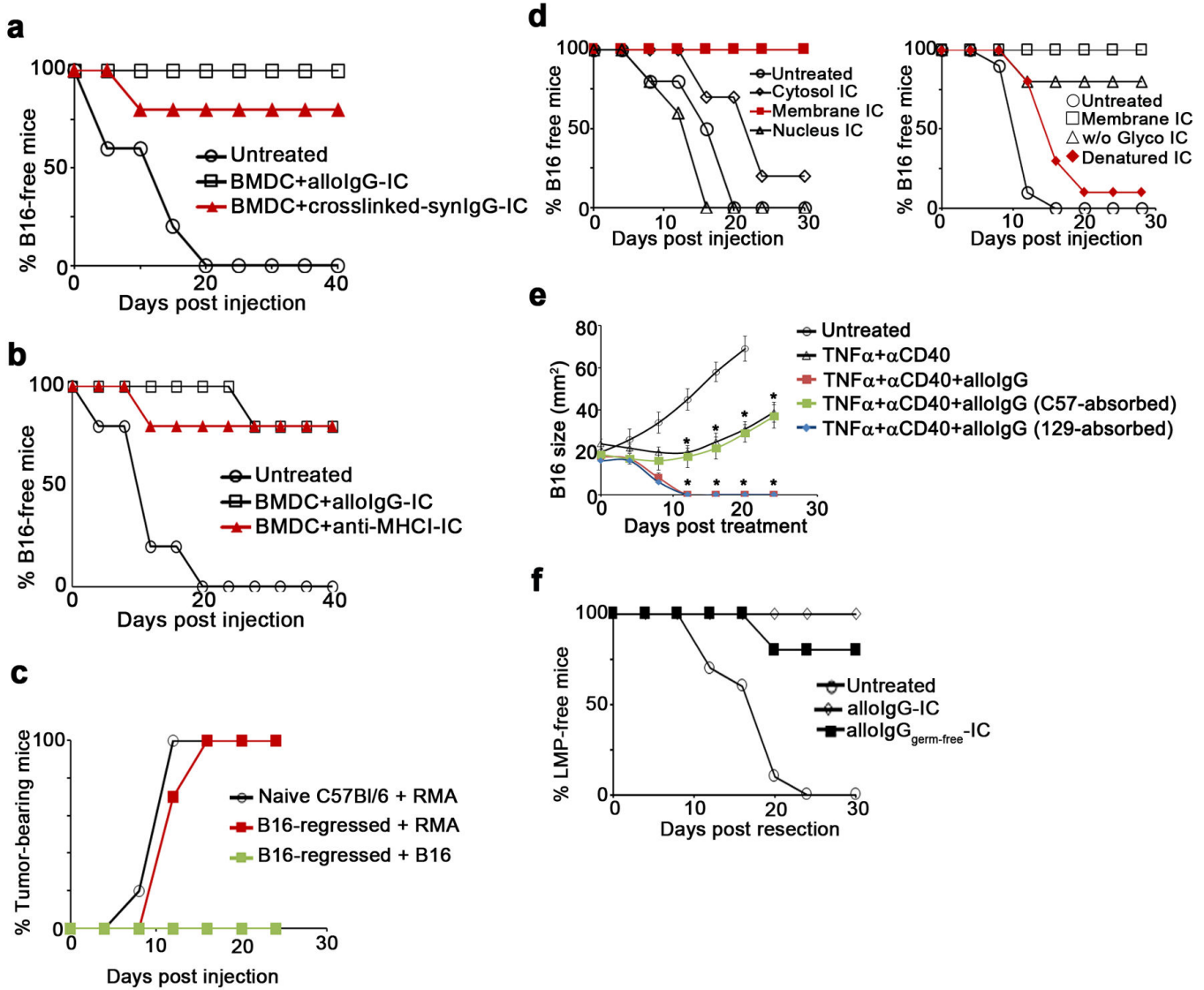
a. Sorting and culture schema of DC from BM and tumor. **b.** Mean levels of IL-12 (left graph) and TNFα (right graph) in the supernatants of DC cultured overnight in medium alone (open bars), with B16 lysates (□), or with alloIgG-IC (■) (n=6). **c.** Percentage of MHCII⁺/CD86⁺ cells (left panel) or CFSE levels (right panel) in tumor-associated DC following overnight activation with PBS (□) or CFSE-labeled alloIgG-IC (■) with or without stimulatory molecules (n=12). **d.** Representative flow cytometric analysis and confocal images from one out of three independent experiments of B16-derived DC cultured overnight with CFSE-labeled fixed B16 cells (n=8). Shown are the mean values ±SEM from three independent experiments Asterisk (*) denotes p<0.05 and two asterisks (**) denote p<0.01.



Extended Data 5.

a. B16 tumor size in C57Bl/6 mice left untreated (\circ) or injected intratumorally with 129S1 alloIgG (\diamond), LPS (\square), TNF α +CD28 (\triangle), LPS+alloIgG (\blacksquare) or TNF α +CD28+alloIgG (\blacktriangle) (n=15). **b.** B16 tumor size in C57Bl/6 mice left untreated (\circ) or injected intratumorally with 129S1 alloIgG (\bullet), TNF α (\square), CD28 (\triangle), or CD40L (\diamond) (n=12). **c.** LL/2 tumor size in C57Bl/6 mice left untreated (\circ), or injected intratumorally with 129S1 alloIgG (\bullet), TNF α +CD40L (\square), TNF α +CD28 (\triangle), TNF α +CD40L+129S1 alloIgG (\blacksquare) or TNF α +CD28+129S1 IgG (\blacktriangle) (n=8). **d.** Representative flow cytometric analysis from one out of three independent experiments of IgG binding total myeloid cells in B16 tumor-bearing mice 3 hours after intratumoral injection of PBS or 5 μ g PE-labeled alloIgG. **e.** Total numbers of CD11c⁺ cells in the draining lymph nodes of B16 tumor-bearing mice 4 days after treatment (n=6). **f.** Gating and sorting strategy of immune cell populations infiltrating B16 tumors. **g.** B16 growth in mice vaccinated with 2 \times 10⁶ B cells, mast cells, macrophages or NK cells

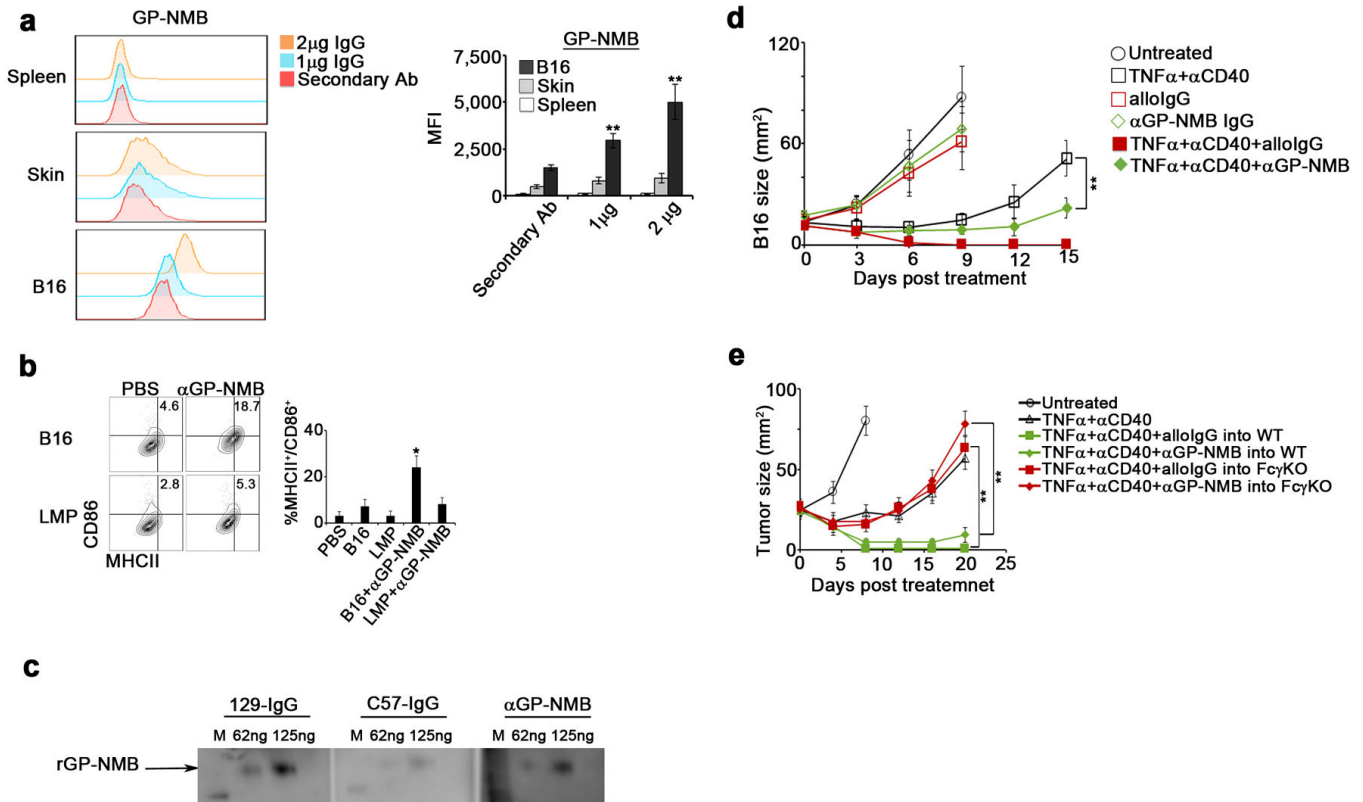
from B16 tumors untreated (○), or injected with alloIgG (□) or alloIgG+TNF α + α CD40 (◇) (n=6). Shown are the mean values \pm SEM from two independent experiments. Asterisk (*) denotes p<0.05 and two asterisks (**) denote p<0.01.



Extended Data 6.

a. B16 frequency in mice untreated (○), or treated with BMDC loaded with intact B16 cells coated with alloIgG (□), or with intact B16 cells cross-linked to syngeneic IgG (▲) (n=8). **b.** B16 tumor frequency in mice untreated (○) or treated with BMDC loaded with intact B16 cells coated with alloIgG (□) or with intact B16 coated with monoclonal IgG against MHC-I (▲) (n=8). **c.** RMA tumor growth following inoculation with 2.5×10^5 tumor cells in naïve C57Bl/6 mice (○), or in C57Bl/6 mice in which B16 tumors had completely regressed following treatment with alloIgG+TNF α + α CD40 (■). Also shown is the lack of B16 tumor growth in C57Bl/6 mice that were re-challenged with 2×10^5 B16 tumor cells following the regression of this tumor after treatment with alloIgG+TNF α + α CD40 (■) (n=8). **d.** Left:

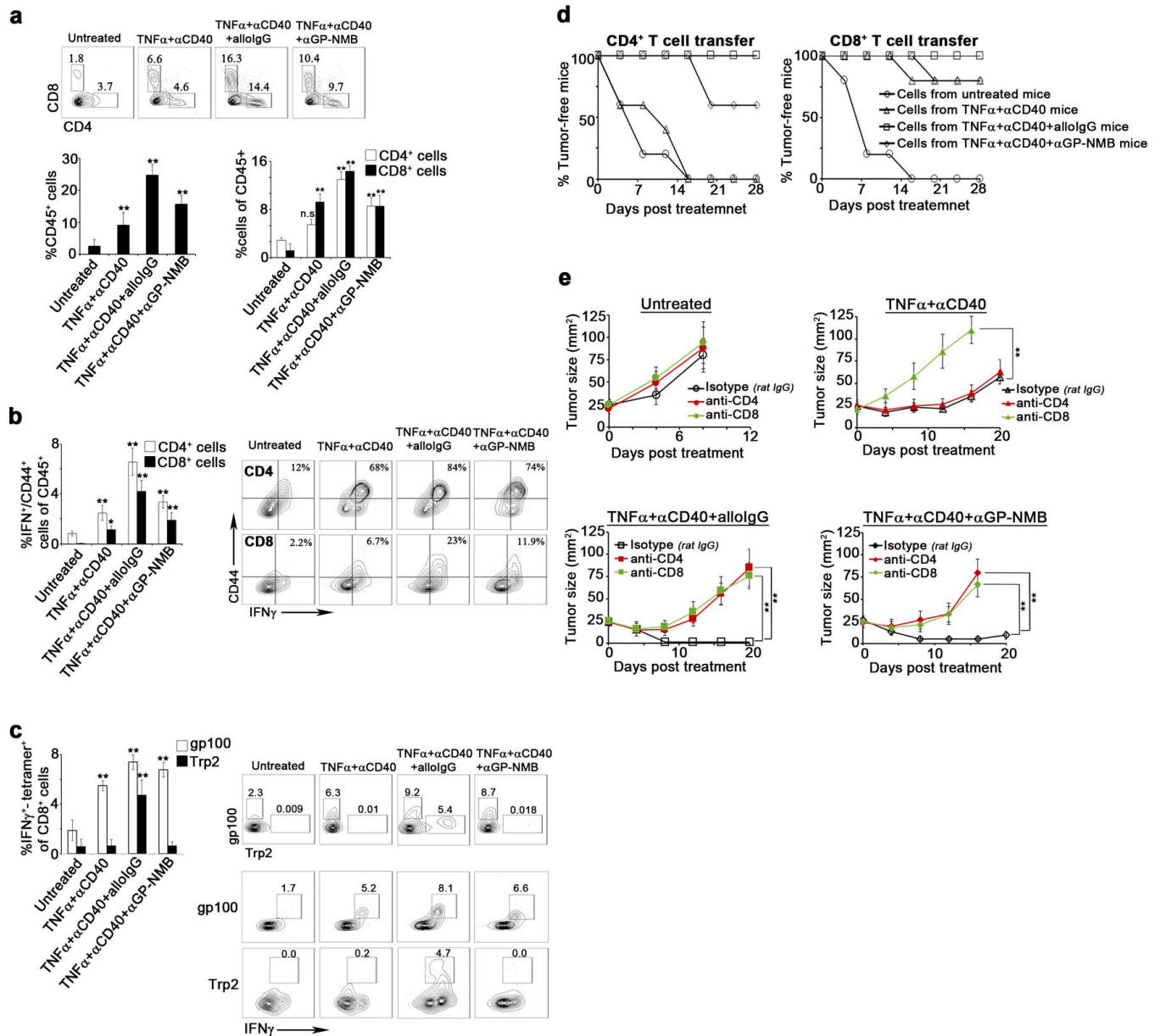
Tumor frequency in mice untreated (○) or treated with DC loaded with IC formed with alloIgG and cytosolic tumor proteins (◇), nuclear tumor proteins (△) or membrane tumor proteins (■). Right: Tumor frequency in mice untreated (○), treated with DC loaded with IC formed from alloIgG and membrane proteins (□), membrane proteins without O- and N-glycans (△), or heat-denatured membrane proteins (◆) (n=5). **e.** B16 tumor growth in C57Bl/6 mice untreated (○), or injected with TNF α + α CD40 (△), TNF α + α CD40+alloIgG (■), or TNF α + α CD40 and alloIgG absorbed on normal cells of the IgG-donor background (◆) or on normal cells of the tumor background (■) (n=6). **f.** Tumor recurrence rates following resection in mice left untreated (○), treated with 2×10^6 DC loaded with IgG-IC from conventionally-raised C57Bl/6 (◇), or with 2×10^6 DC loaded with IgG-IC from gnotobiotic C57Bl/6 mice (■) (n=6). Shown are the mean values \pm SEM from two independent experiments. Asterisk (*) denotes $p < 0.05$ and two asterisks (**) denote $p < 0.01$.



Extended Data 7.

a. Representative flow cytometric analysis and quantitation of binding of anti-IgG secondary antibody alone (■), 1 μ g anti-GP-NMB (■) or 2 μ g GP-NMB (■) per 1×10^5 B16 cells, normal skin cells, or normal spleen cells (n=6). **b.** Percentage of MHCII⁺/CD86⁺ BMDC following overnight activation with untreated LMP or B16 tumor cells, or with tumor cells coated with anti-GP-NMB (2μ g/ 1×10^5 tumor cells) (n=8). **c.** Western blot of recombinant GP-NMB (62.5 ng and 125 ng) performed with 10 μ g/mL of IgG from naïve 129S1 mice, naïve C57Bl/6 mice, or 1 μ g/mL α GP-NMB. **d.** B16 tumor size in mice untreated (○) or treated with TNF α + α CD40 (□), alloIgG (■), anti-GP-NMB IgG (◇), TNF α

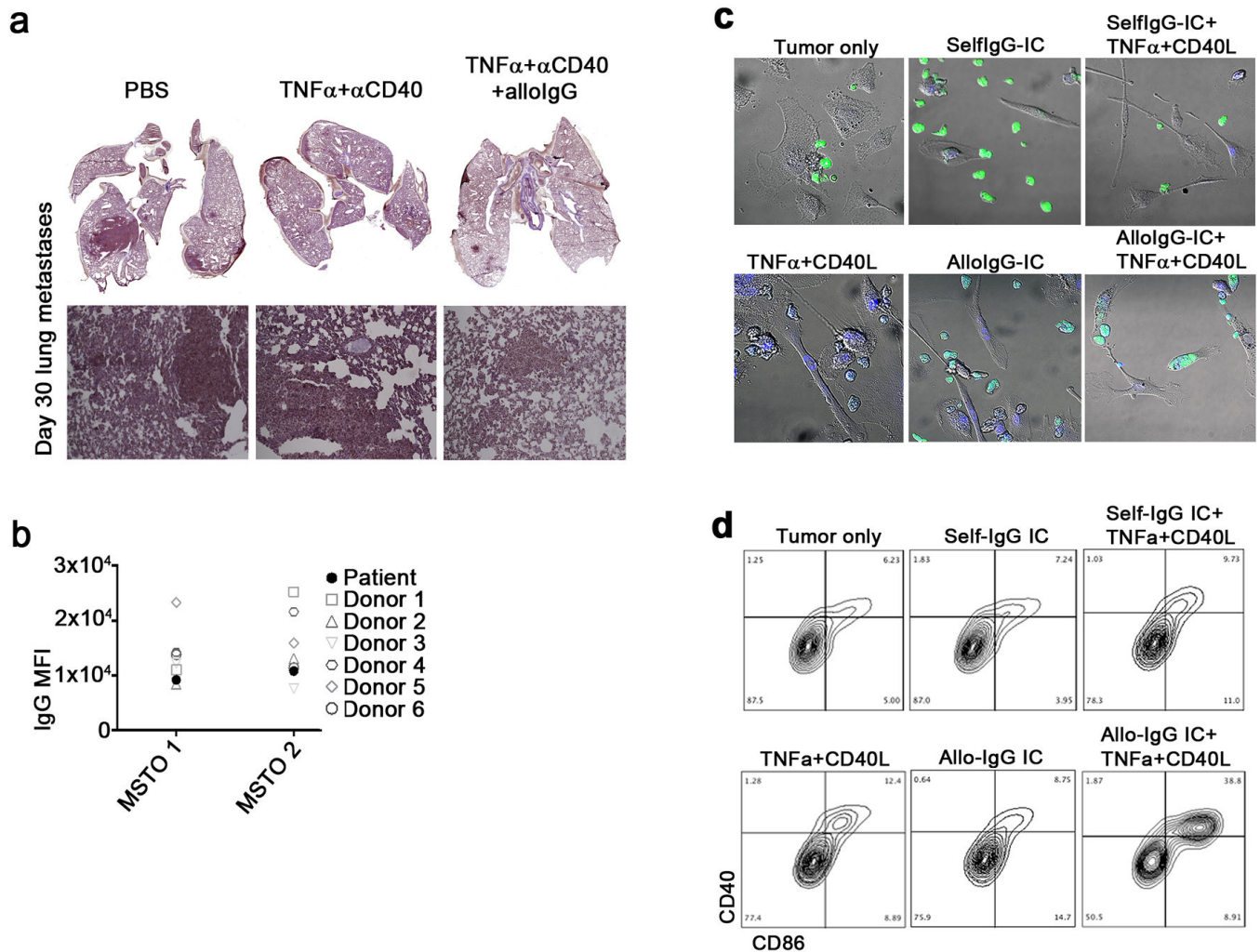
+ α CD40+alloIgG (■), or with TNF α + α CD40+ α GP-NMB (◆) (n=8). e. B16 tumor size in C57Bl/6 WT mice untreated (○) or treated with TNF α + α CD40 (Δ), TNF α + α CD40+alloIgG (■), or with TNF α + α CD40+anti-GP-NMB (◆), or in Fc γ R KO mice treated with TNF α + α CD40+alloIgG (■), or with TNF α + α CD40+anti-GP-NMB (◆) (n=8). Shown are the mean values \pm SEM from two independent experiments. Asterisk (*) denotes $p < 0.05$ and two asterisks (**) denote $p < 0.01$.



Extended Data 8.

a. Representative flow cytometry plots of CD4⁺ and CD8⁺ cells in B16 tumors 6 days following treatment. Left graph: Percentage of CD45⁺ cells infiltrating B16 tumors 15–17 days after s.c. inoculation or six days after treatment. Right graph: Percentage of CD4⁺ (□)

and CD8⁺ cells (■) among tumor-infiltrating CD45⁺ cells (n=10). **b.** Percentages of CD44 and IFN γ co-expressing CD4⁺ (□) and CD8⁺ cells (■) among tumor-infiltrating CD45⁺ cells 6 days following treatment or 15 days following s.c. inoculation (n=10) **c.** Frequency of IFN γ -expressing T cells that recognize gp100 (□) and Trp2 (■) among day 6 post-treatment tumor-infiltrating CD8⁺ cells. Gate shown: CD8⁺ T cells (n=10). **d.** Percentage of tumor-free mice following adoptive transfer of T cells from day 6 post-treatment B16 tumor-bearing mice untreated (○), treated with TNF α + α CD40 (Δ), with TNF α + α CD40+alloIgG (□), or with TNF α + α CD40+ α GP-NMB (◇). (n=9). **e.** Upper left: B16 tumor growth in untreated C57Bl/6 mice injected with rat IgG (○), with rat anti-CD4 (●), or with rat-CD8 (●). Upper right: B16 tumor growth in C57Bl/6 mice treated with TNF α + α CD40 and injected with rat IgG (Δ), with rat anti-CD4 (▲), or with rat-CD8 (▲). Lower left: B16 growth in C57Bl/6 mice treated with TNF α + α CD40+alloIgG and injected with rat IgG (□), with rat anti-CD4 (■), or with rat-CD8 (■). Lower right: B16 growth in C57Bl/6 mice treated with TNF α + α CD40+ α GP-NMB and injected with rat IgG (◇), with rat anti-CD4 (◆), or with rat-CD8 (◆) (n=9). Shown are the mean values \pm SEM from three independent experiments. Asterisk (*) denotes p<0.05 and two asterisks (**) denote p<0.01.



Extended Data 9.

a. Representative H&E sections of lung metastases on day 30 from one out of three independent experiments performed (magnification: 10x). **b.** MFI of tumor cells from MSTO-resected patients coated with autologous IgG or IgG from healthy donors (n=6). **c and d.** Widefield microscopy (c) and flow cytometry plots (d) of TADC from a lung carcinoma patient incubated overnight with autologous CFSE-labeled tumor cells (green) coated with selfIgG or alloIgG derived from a pool of 10 donors ($1\mu\text{g}/2 \times 10^5$ cells) and in the presence of 50 ng/mL $TNF\alpha$ and 1 $\mu\text{g}/\text{mL}$ CD40L. Shown are the mean values \pm SEM from two independent experiments. Asterisk (*) denotes $p < 0.05$ and two asterisks (**) denote $p < 0.01$.

Extended Data Table 1

a.-c. 20 µg of native cell membrane proteins were incubated with 50 µg of syngeneic (C57Bl/6) or allogeneic (129S1) IgG coupled to protein G magnetic beads and precipitated proteins were analyzed by mass-spectrometry. Tables show the conversion to Spectral Abundance Factor (SAF) and subsequent Normalized Spectral Abundance Factor (NSAF). This was based on the equation: NSAF = (SpC/MW)/Σ(SpC/MW)N. Where SpC = Spectral Counts, MW = Protein MW in kDa and N = Total Number of Proteins.

a. Proteins enriched by alloIgG		Accession Number	C57 SpC	129 SpC	C57 SAF	129 SAF	C57 NSAF	129 NSAF	C57/129 ratio
Endoplasmic reticulum membrane									
1	Transmembrane protein 93	sp Q9CQW0 TMM93_MOUSE	0	2	0	0.166667	0	0.0007367	2
2	Endoplasmic reticulum-Golgi intermediate compartment protein 3	sp Q9CQE7 ERGI3_MOUSE	0	2	0	0.046512	0	0.00020559	2
3	Reticulon-4	sp Q99P72 RTN4_MOUSE	0	2	0	0.015748	0	6.9609E-05	2
4	Uncharacterized protein C12orf41 homolog	sp Q8BQR4 CL041_MOUSE	0	2	0	0.037037	0	0.00016371	2
5	Erlin-2	sp Q8BFZ9 ERLN2_MOUSE	0	2	0	0.052632	0	0.00023264	2
6	Transitional endoplasmic reticulum ATPase	sp Q01853 TERA_MOUSE	0	2	0	0.022472	0	9.933E-05	2
7	Dolichyl-diphosphooligosaccharide--protein glycosyltransferase subunit DAD1	sp P61804 DADI_MOUSE	0	2	0	0.166667	0	0.0007367	2
8	Calnexin	sp P35564 CALX_MOUSE	0	2	0	0.029851	0	0.00013195	2
9	Calumenin	sp O35887 CALU_MOUSE	0	2	0	0.054054	0	0.00023893	2
10	Vesicle-associated membrane protein-associated protein A	sp Q9WV55 VAPA_MOUSE	0	3	0	0.107143	0	0.00047359	3
11	Mannosyl-oligosaccharide glucosidase	sp Q80UM7 MOGS_MOUSE	0	3	0	0.032609	0	0.00014414	3
12	Neutral alpha-glucosidase	sp Q8BHN3 GANAB_MOUSE	0	3	0	0.028037	0	0.00012393	3
13	ERO1-like protein alpha	sp Q8R180 ERO1A_MOUSE	0	5	0	0.092593	0	0.00040928	5
14	UDP-glucose:glycoprotein glucosyltransferase 1	sp Q6P5E4 UGGG1_MOUSE	0	5	0	0.028409	0	0.00012557	5
15	Prolyl 4-hydroxylase subunit alpha-1	sp Q60715 P4HA1_MOUSE	0	5	0	0.081967	0	0.00036231	5
16	Epoxide hydrolase 1	sp Q9D379 HYEP_MOUSE	0	9	0	0.169811	0	0.0007506	9
17	Calreticulin	sp P14211 CALR_MOUSE	0	14	0	0.291667	0	0.00128922	14
18	Sarcoplasmic/endoplasmic reticulum calcium ATPase	sp O55143 AT2A2_MOUSE	8	18	0.06956522	0.156522	0.0003684	0.00069185	1.8782025
19	Protein disulfide-isomerase A4	sp P08003 PDI4_MOUSE	0	12	0	0.166667	0	0.0007367	12
20	Protein disulfide-isomerase	sp P09103 PDI1_MOUSE	0	12	0	0.210526	0	0.00093056	12

a. Proteins enriched by alloIgG										
Identified Proteins	Accession Number	C57 SpC	129 SpC	C57 SAF	129 SAF	C57 NSAF	129 NSAF	C57/129 ratio		
21 Protein disulfide-isomerase A3	sp P27773 PDIA3_MOUSE	0	9	0	0.157895	0	0.00069792	9		
22 Protein disulfide-isomerase A6	sp Q922R8 PDIA6_MOUSE	0	11	0	0.229167	0	0.00101296	11		
Melanosomes and vesicles membranes										
1 Peptidyl-prolyl cis-trans isomerase B	sp P24369 PP1B_MOUSE	0	7	0	0.291667	0	0.00128922	7		
Cell membrane										
1 T-complex protein 1 subunit gamma	sp P80318 ITCPG_MOUSE	0	2	0	0.032787	0	0.00014492	2		
2 Monocarboxylate transporter 4	sp P57787 MOT4_MOUSE	0	2	0	0.04	0	0.00017681	2		
3 Nicastatin	sp P57716 NICA_MOUSE	0	2	0	0.025641	0	0.00011334	2		
4 Basigin	sp P18572 BASI_MOUSE	0	2	0	0.047619	0	0.00021048	2		
5 Vesicle-associated membrane protein-associated protein A	sp Q9WV55 VAPA_MOUSE	0	3	0	0.107143	0	0.00047359	3		
6 Retrovirus-related Env polyprotein from Fv-4	sp P11370 ENV2_MOUSE	0	3	0	0.040541	0	0.0001792	3		
7 Synaptic vesicle membrane protein	sp Q62465 VAT1_MOUSE	0	4	0	0.093023	0	0.00041118	4		
8 4F2 cell-surface antigen heavy chain	sp P10852 4F2_MOUSE	0	4	0	0.068966	0	0.00030484	4		
9 Alpha-enolase	sp P17182 ENOA_MOUSE	0	5	0	0.106383	0	0.00047023	5		
10 Integrin-linked protein kinase	sp O55222 ILK_MOUSE	0	4	0	0.078431	0	0.00034668	4		
11 Transmembrane glycoprotein NMB	sp Q99P91 GNMB_MOUSE	2	15	0.03125	0.234375	0.0001655	0.00103598	6.2606749		
12 MLV-related proviral Env polyprotein	sp P10404 ENV1_MOUSE	0	13	0	0.185714	0	0.00082089	13		
13 ERO1-like protein alpha	sp Q8R180 ERO1A_MOUSE	0	5	0	0.092593	0	0.00040928	5		
14 Clathrin heavy chain 1	sp Q68FD5 CLH_MOUSE	0	5	0	0.026042	0	0.00011511	5		
15 Desmoglein-1-alpha	sp Q61495 DSG1A_MOUSE	2	5	0.0173913	0.043478	9.209E-05	0.00019218	2.0868916		
16 Sodium/potassium-transporting ATPase subunit alpha-1	sp Q8VDN2 AT1A1_MOUSE	4	12	0.035539823	0.106195	0.0001874	0.0004694	2.50427		

b. Proteins equally enriched by symIgG and alloIgG										
Identified Proteins	Accession Number	C57 SpC	129 SpC	C57 SAF	129 SAF	C57 NSAF	129 NSAF	C57/129 ratio		
Endoplasmic reticulum membrane										
1 DnaJ homolog subfamily B member 11	sp Q99KV1 DJB11_MOUSE	8	6	0.19512195	0.146341	0.0010332	0.00064686	0.6260675		
2 78 kDa glucose-regulated protein	sp P20029 GRP78_MOUSE	73	71	1.01388889	0.986111	0.0053687	0.00435879	0.8118866		
3 Serpin H1	sp P19524 SERPH_MOUSE	11	17	0.23404255	0.361702	0.0012393	0.00159879	1.2900785		

b. Proteins equally enriched by synIgG and allIgG

Identified Proteins	Accession Number	C57 SpC	129 SpC	C57 SAF	129 SAF	C57 NSAF	129 NSAF	C57/129 ratio
Endoplasmic reticulum membrane								
4 Protein transport protein Sec61 subunit beta	sp Q9CQS8 SC61B_MOUSE	2	3	0.2	0.3	0.001059	0.00132605	1.252135
5 Leucine-rich repeat-containing protein 59	sp Q922Q8 LRC59_MOUSE	3	2	0.08571429	0.057143	0.0004539	0.00025258	0.5565044
6 Protein transport protein Sec61 subunit alpha isoform 1	sp P61620 S61A1_MOUSE	9	10	0.17307692	0.192308	0.0009165	0.00085003	0.9275074
7 Dolichyl-diphosphooligosaccharide--protein glycosyltransferase 48 kDa subunit	sp O54734 OST48_MOUSE	3	5	0.06122449	0.102041	0.0003242	0.00045104	1.3912611
8 Estradiol 17-beta-dehydrogenase 12	sp O70503 DHB12_MOUSE	7	6	0.2	0.171429	0.001059	0.00075774	0.7155057
Melanosomes and vesicles membranes								
1 Flotillin-2	sp Q60634 FLOT2_MOUSE	3	2	0.06382979	0.042553	0.000338	0.00018809	0.5565044
2 Cathepsin D	sp P18242 CATD_MOUSE	3	5	0.06666667	0.111111	0.000353	0.00049113	1.3912611
3 AP-2 complex subunit beta	sp Q9DBG3 AP2B1_MOUSE	8	5	0.07619048	0.047619	0.0004034	0.00021048	0.5217229
4 AP-2 complex subunit mu	sp P84091 AP2M1_MOUSE	4	5	0.08	0.1	0.0004236	0.00044202	1.0434458
5 Annexin A2	sp P07356 ANXA2_MOUSE	4	6	0.1025641	0.153846	0.0005431	0.00068003	1.252135
6 Melanocyte protein PMEL	sp Q60696 PMEL_MOUSE	5	4	0.07575758	0.060606	0.0004011	0.00026789	0.6678053
Cell membrane								
1 Desmoplakin	sp E9Q557 DESP_MOUSE	63	60	0.18918919	0.18018	0.0010018	0.00079643	0.7950063
2 PDZ domain	sp Q9Z0G0 GIPC1_MOUSE	13	9	0.36111111	0.25	0.0019121	0.00110504	0.5779085
3 Junction plakoglobin	sp Q02257 PLAK_MOUSE	37	49	0.45121951	0.597561	0.0023893	0.00264133	1.1054885

c. Proteins enriched by synIgG

Identified Proteins	Accession Number	C57 SpC	129 SpC	C57 SAF	129 SAF	C57 NSAF	129 NSAF	C57/129 ratio
Endoplasmic reticulum membrane								
1 Stromal cell-derived factor 2-like protein 1	sp Q9ESP1 SDF2L_MOUSE	3	0	0.125	0	0.0006619	0	3
2 Nicotin	sp Q8VCM8 NCLN_MOUSE	2	0	0.03174603	0	0.0001681	0	2
3 Translocation protein SEC62	sp Q8BU14 SEC62_MOUSE	4	0	0.08695652	0	0.0004604	0	4
4 Disco-interacting protein 2 homolog B	sp Q3UH60 DIP2B_MOUSE	4	0	0.02339181	0	0.0001239	0	4
melanosomes and Vesicles membranes								
1 Vacuolar protein sorting-associated protein 35	sp Q9EQH3 VPS35_MOUSE	2	0	0.02173913	0	0.0001151	0	2
2 Angiomotin-like protein 2	sp Q8K371 AMOL2_MOUSE	6	0	0.07058824	0	0.0003738	0	6

c. Proteins enriched by synIgG									
Identified Proteins	Accession Number	C57 SpC	129 SpC	C57 SAF	129 SAF	C57 NSAF	129 NSAF	C57/129 ratio	
Endoplasmic reticulum membrane									
3 Fibrous sheath-interacting protein 2	sp A2ARZ3 FSIP2_MOUSE	9	0	0.01146497	0	6.071E-05	0	9	
Cell membrane									

Supplementary Material

Refer to Web version on PubMed Central for supplementary material.

Acknowledgments

The authors thank Dr. F. Carl Grumet and Dr. Nathan E. Reticker-Flynn for helpful discussion. We also thank Dr. Justin Sonnenburg for providing gnotobiotic mice. This work was supported by NIH grants U01 CA141468 and 5T32AI007290-27. M.H.S. is supported by NIH NRSA F31CA189331. I.L.L. is supported by a Smith Stanford Graduate Fellowship.

References

1. Coussens LM, Zitvogel L, Palucka AK. Neutralizing tumor-promoting chronic inflammation: a magic bullet? *Science*. 2013; 339:286–291. [PubMed: 23329041]
2. Grivnennikov SI, Greten FR, Karin M. Immunity, inflammation, and cancer. *Cell*. 2010; 140:883–899. [PubMed: 20303878]
3. Hanahan D, Coussens LM. Accessories to the crime: functions of cells recruited to the tumor microenvironment. *Cancer cell*. 2012; 21:309–322. [PubMed: 22439926]
4. Schreiber RD, Old LJ, Smyth MJ. Cancer immunoeediting: integrating immunity's roles in cancer suppression and promotion. *Science*. 2011; 331:1565–1570. [PubMed: 21436444]
5. Vesely MD, Kershaw MH, Schreiber RD, Smyth MJ. Natural innate and adaptive immunity to cancer. *Annual review of immunology*. 2011; 29:235–271.
6. Manning TC, et al. Antigen recognition and allogeneic tumor rejection in CD8+ TCR transgenic/RAG(–/–) mice. *Journal of immunology*. 1997; 159:4665–4675.
7. Ferrara J, Guillen FJ, Sleckman B, Burakoff SJ, Murphy GF. Cutaneous acute graft-versus-host disease to minor histocompatibility antigens in a murine model: histologic analysis and correlation to clinical disease. *J Invest Dermatol*. 1986; 86:371–375. [PubMed: 3528309]
8. Appelbaum FR. Haematopoietic cell transplantation as immunotherapy. *Nature*. 2001; 411:385–389. [PubMed: 11357147]
9. Bishop MR, et al. Allogeneic lymphocytes induce tumor regression of advanced metastatic breast cancer. *J Clin Oncol*. 2004; 22:3886–3892. [PubMed: 15314059]
10. Goulmy E. Minor histocompatibility antigens: allo target molecules for tumor-specific immunotherapy. *Cancer J*. 2004; 10:1–7. [PubMed: 15000488]
11. Tseng WW, et al. Development of an orthotopic model of invasive pancreatic cancer in an immunocompetent murine host. *Clinical cancer research : an official journal of the American Association for Cancer Research*. 2010; 16:3684–3695. [PubMed: 20534740]
12. Dankort D, et al. Braf(V600E) cooperates with Pten loss to induce metastatic melanoma. *Nat Genet*. 2009; 41:544–552. [PubMed: 19282848]
13. Qin Z, et al. B cells inhibit induction of T cell-dependent tumor immunity. *Nature medicine*. 1998; 4:627–630.
14. de Visser KE, Korets LV, Coussens LM. De novo carcinogenesis promoted by chronic inflammation is B lymphocyte dependent. *Cancer cell*. 2005; 7:411–423. [PubMed: 15894262]
15. Andreu P, et al. FcRgamma activation regulates inflammation-associated squamous carcinogenesis. *Cancer cell*. 2010; 17:121–134. [PubMed: 20138013]
16. Gerber JS, Mosser DM. Reversing lipopolysaccharide toxicity by ligating the macrophage Fc gamma receptors. *Journal of immunology*. 2001; 166:6861–6868.
17. Willimsky G, et al. Immunogenicity of premalignant lesions is the primary cause of general cytotoxic T lymphocyte unresponsiveness. *The Journal of experimental medicine*. 2008; 205:1687–1700. [PubMed: 18573907]
18. Soussi T. p53 Antibodies in the sera of patients with various types of cancer: a review. *Cancer research*. 2000; 60:1777–1788. [PubMed: 10766157]
19. Gumus E, et al. Association of positive serum anti-p53 antibodies with poor prognosis in bladder cancer patients. *International journal of urology : official journal of the Japanese Urological Association*. 2004; 11:1070–1077. [PubMed: 15663677]
20. Li Q, et al. Adoptive transfer of tumor reactive B cells confers host T-cell immunity and tumor regression. *Clinical cancer research : an official journal of the American Association for Cancer Research*. 2011; 17:4987–4995. [PubMed: 21690573]

21. DiLillo DJ, Yanaba K, Tedder TF. B cells are required for optimal CD4+ and CD8+ T cell tumor immunity: therapeutic B cell depletion enhances B16 melanoma growth in mice. *Journal of immunology*. 2010; 184:4006–4016.
22. Clynes R, Takechi Y, Moroi Y, Houghton A, Ravetch JV. Fc receptors are required in passive and active immunity to melanoma. *Proceedings of the National Academy of Sciences of the United States of America*. 1998; 95:652–656. [PubMed: 9435247]
23. Nimmerjahn F, Ravetch JV. Divergent immunoglobulin g subclass activity through selective Fc receptor binding. *Science*. 2005; 310:1510–1512. [PubMed: 16322460]
24. Hamanaka Y, et al. Circulating anti-MUC1 IgG antibodies as a favorable prognostic factor for pancreatic cancer. *International journal of cancer. Journal international du cancer*. 2003; 103:97–100. [PubMed: 12455059]
25. Kurtenkov O, et al. Humoral immune response to MUC1 and to the Thomsen-Friedenreich (TF) glycotope in patients with gastric cancer: relation to survival. *Acta Oncol*. 2007; 46:316–323. [PubMed: 17450466]
26. Schuurhuis DH, et al. Immune complex-loaded dendritic cells are superior to soluble immune complexes as antitumor vaccine. *Journal of immunology*. 2006; 176:4573–4580.
27. Regnault A, et al. Fcγ receptor-mediated induction of dendritic cell maturation and major histocompatibility complex class I-restricted antigen presentation after immune complex internalization. *The Journal of experimental medicine*. 1999; 189:371–380. [PubMed: 9892619]
28. Rafiq K, Bergtold A, Clynes R. Immune complex-mediated antigen presentation induces tumor immunity. *The Journal of clinical investigation*. 2002; 110:71–79. [PubMed: 12093890]
29. Schachter J, et al. Efficacy and safety of intravenous immunoglobulin in patients with metastatic melanoma. *Ann N Y Acad Sci*. 2007; 1110:305–314. [PubMed: 17911445]
30. Fishman P, Bar-Yehuda S, Shoenfeld Y. IVIg to prevent tumor metastases (Review). *Int J Oncol*. 2002; 21:875–880. [PubMed: 12239629]

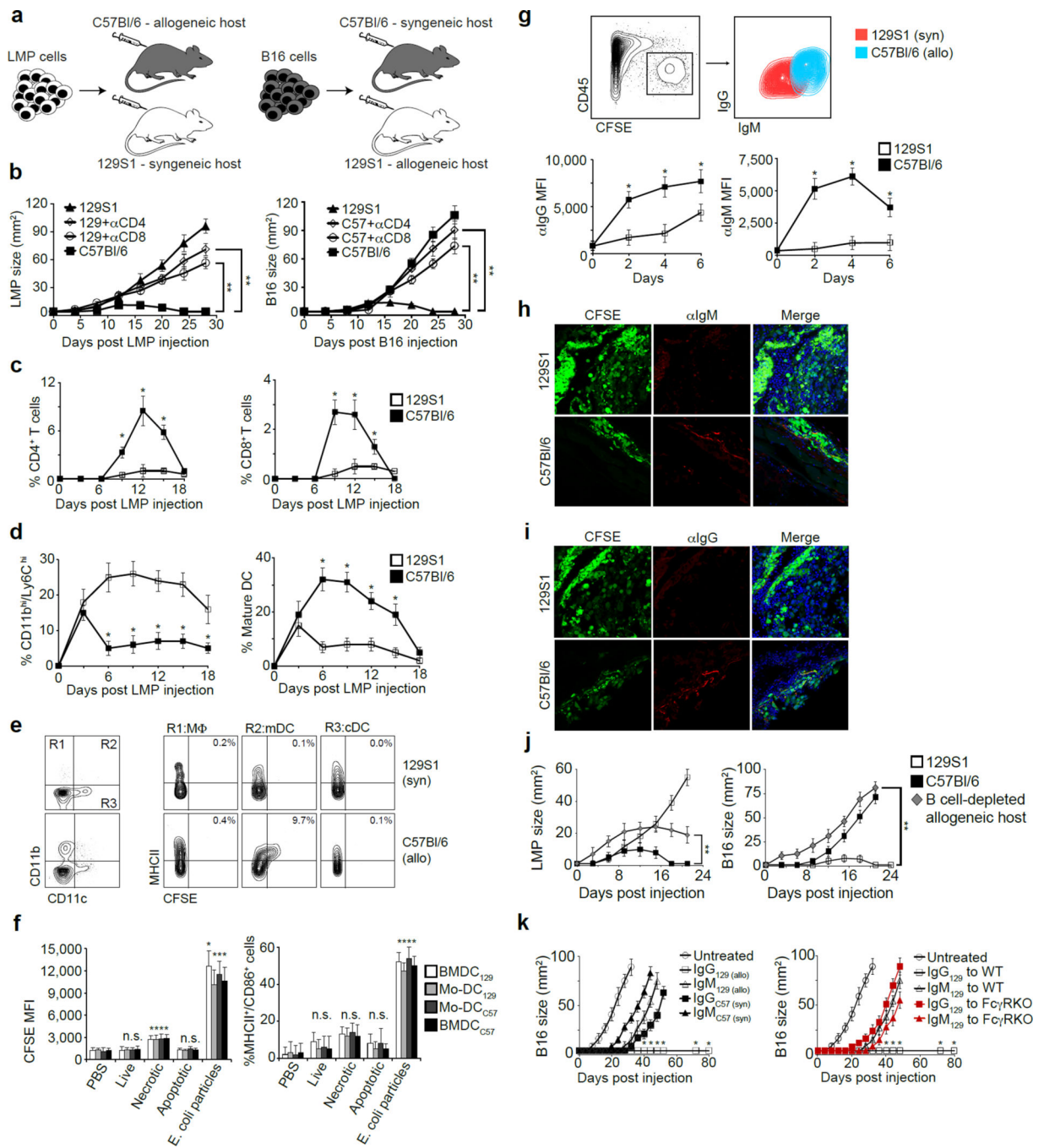


Figure 1. Tumor-binding antibodies initiate rejection of allogeneic tumors

a. Experimental design: Injection of LMP and B16 cells s.c. into syngeneic and allogeneic hosts. **b.** Growth of LMP and B16 tumors in C57Bl/6, 129S1, CD4⁺ cell-depleted or CD8⁺ cell-depleted allogeneic mice (n=6). **c.** Percentages of LMP-infiltrating CD4⁺ and CD8⁺ T cells among CD45⁺ cells (n=5). **d.** Percentages of LMP-infiltrating CD11b^{hi}/Ly6C^{hi} cells and mature DC among total cells (n=4). **e.** Myeloid cells in the draining lymph nodes of mice inoculated with CFSE-labeled LMP cells 3d earlier (n=5). **f.** Tumor uptake, MHCII and CD86 expression by BMDC and blood monocyte-derived (Mo)-DC incubated overnight

with CFSE-labeled live, frozen/thawed (necrotic), or mitomycin C-treated (apoptotic) LMP cells or fluorescein-labeled *E. coli* BioParticles (n=4). **g.** IgG and IgM bound *in vivo* to CFSE-labeled LMP cells 48h after tumor inoculation (n=5). **h. and i.** Representative staining of tumor sections by IgM and IgG 24h following inoculation of CFSE-labeled LMP cells. **j.** Tumor size in 129S1, C57Bl/6 and B cell-depleted allogeneic hosts (n=5). **k.** B16 size in naive mice or mice injected with syngeneic or allogeneic antibodies (n=5). B16 size in naïve C57Bl/6 and Fc γ R KO mice injected with allogeneic antibodies (n=5). Experiments were independently repeated at least 3 times and analyzed by Mann–Whitney U test. Asterisk (*) denotes p<0.05 and two asterisks (**) denote p<0.01.

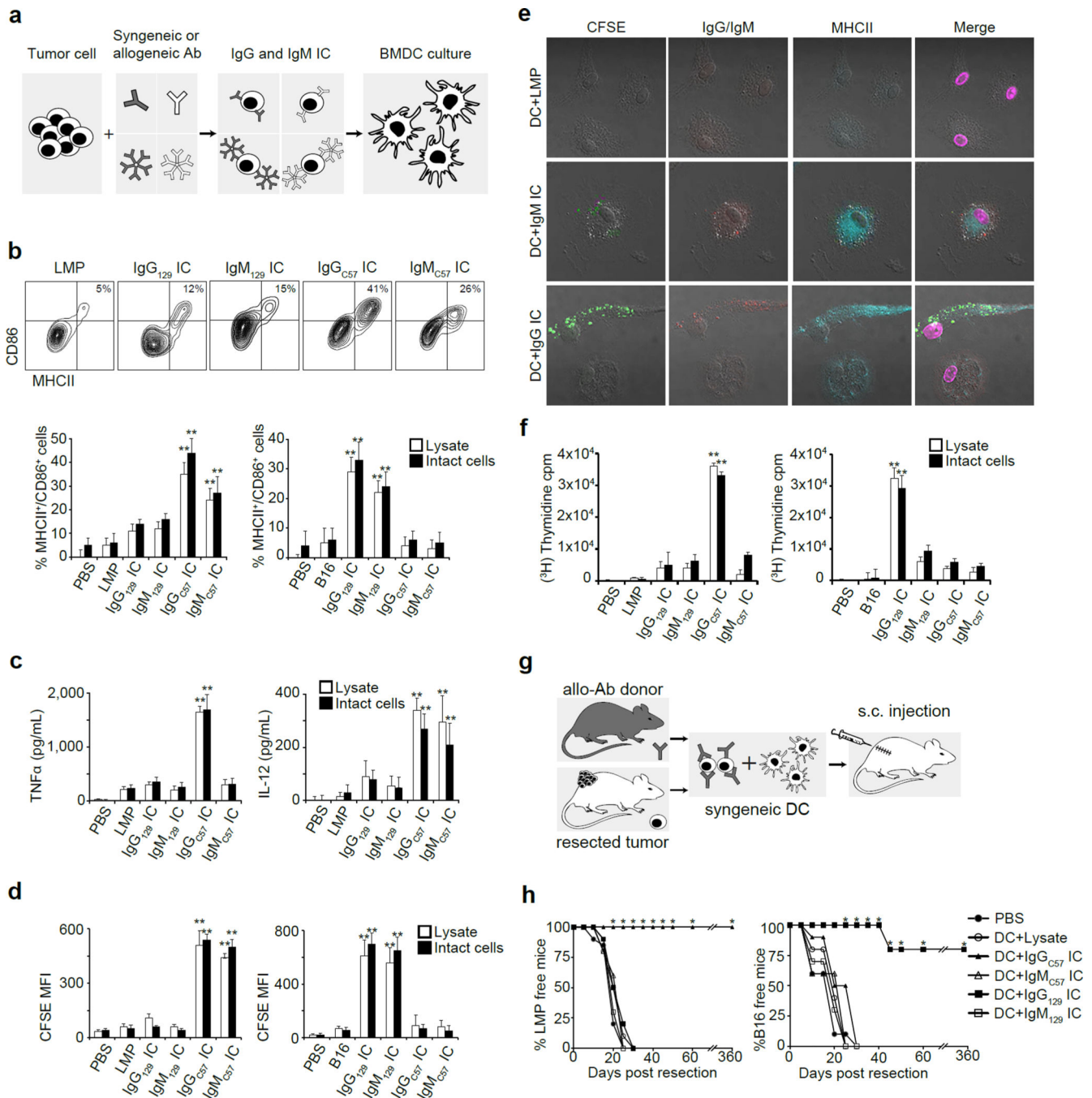


Figure 2. AlloIgG-IC are internalized and presented by BMDC and drive protective immunity *in vivo*

a. Experimental design: Tumor cells or lysates were incubated with syngeneic or allogeneic antibodies and then cultured with BMDC overnight. **b.** Expression of CD86/MHCII on BMDC cultured with antibody-coated tumor lysates or intact tumor cells (n=5). **c.** TNF α and IL-12 in supernatants of BMDC cultured overnight with Ig-IC formed with LMP lysate or intact LMP cells (n=5). **d.** Internalization of CFSE in BMDC incubated overnight with Ig-IC formed from CFSE-labeled tumor lysates or CFSE-labeled intact cells (n=4). **e.**

Representative localization of MHCII and Ig-IC on BMDC cultured overnight with CFSE-labeled LMP cells coated with allogeneic antibodies (magnification: 400x). **f.** Proliferation of CD4⁺ T cells cultured with DC loaded with IC formed from LMP and B16 lysates or intact cells (n=5). **g.** Experimental design: Tumors were removed from mice, coated with antibodies, incubated for 24h with BMDC, and injected s.c. into corresponding tumor-resected mice. **h.** Tumor recurrence in mice treated with BMDC loaded with tumor lysate incubated with allogeneic or syngeneic antibodies (n=5). Experiments were independently repeated at least 3 times and analyzed by Mann–Whitney U test. Asterisk (*) denotes p<0.05 and two asterisks (**) denote p<0.01.

Author Manuscript

Author Manuscript

Author Manuscript

Author Manuscript

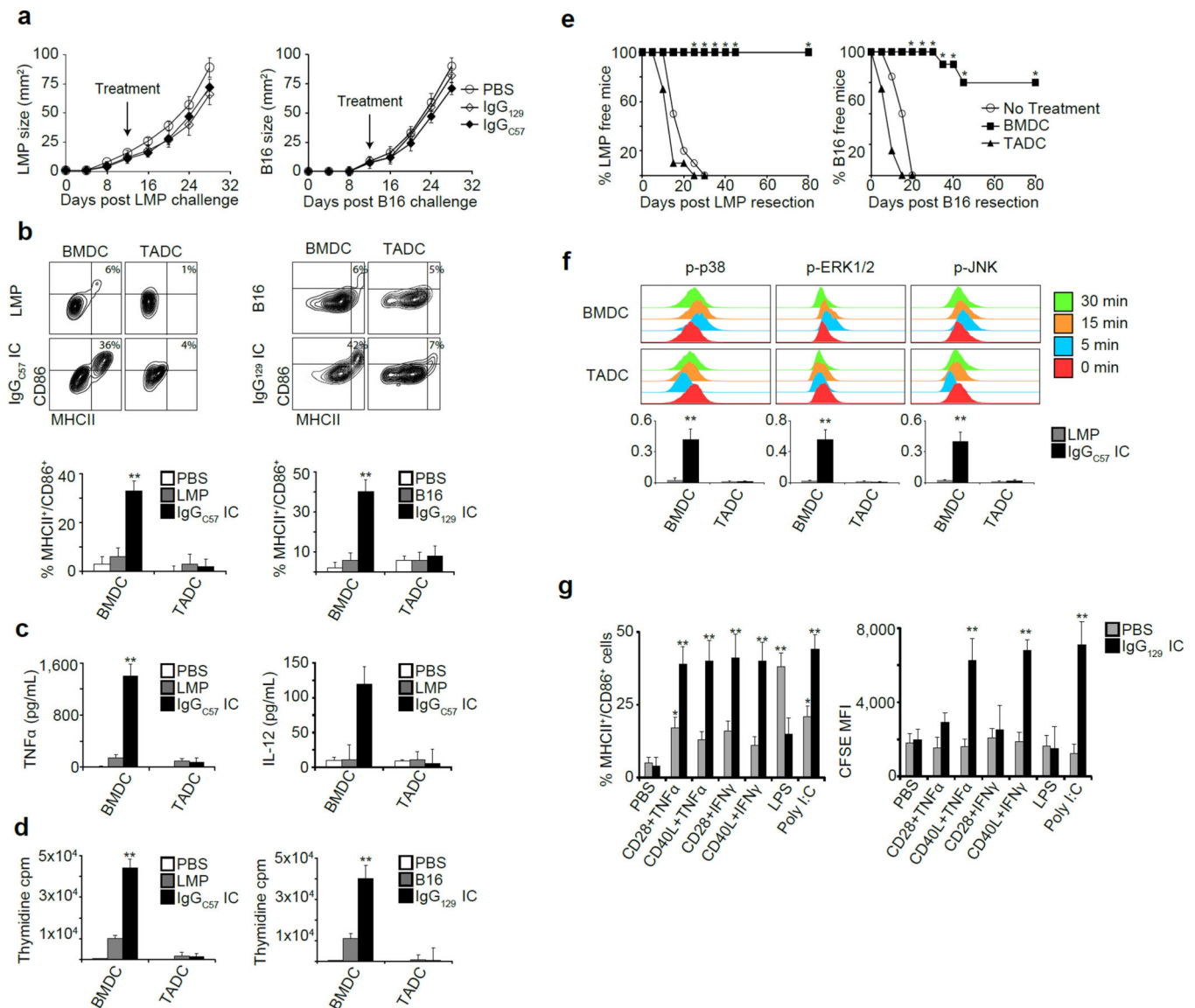


Figure 3. TADC, but not BMDC, require stimulation to respond to alloIgG-IC

a. Tumor growth following intratumoral injection of PBS, 129S1 IgG or C57Bl/6 IgG (n=6).

b. CD86 and MHCII expression on DC incubated with PBS, tumor lysates or alloIgG-IC (n=5).

c. TNFα and IL-12 in the supernatants of DC cultured with PBS control, LMP lysate or alloIgG-IC (n=5).

d. Proliferation of CD4⁺ T cells cultured with DC treated with PBS, tumor lysate, or alloIgG-IC (n=5).

e. Recurrence of resected LMP and B16 in untreated mice or mice treated with alloIgG-IC-activated BMDC or TADC (n=5).

f. p-p38, pERK1/2 and pJNK levels in DC, untreated or incubated with alloIgG-IC. Graphs show arcsinh ratios of phospho-species in DC incubated for 5 min with LMP lysate or alloIgG-IC over baseline levels from unstimulated DC (n=5).

g. MHCII and CD86 expression and CFSE internalization by TADC after overnight culture with CFSE-labeled alloIgG-IC (n=4).

Experiments were independently repeated at least 3 times and analyzed by Mann–Whitney U test. Asterisk (*) denotes $p < 0.05$ and two asterisks (**) denote $p < 0.01$.

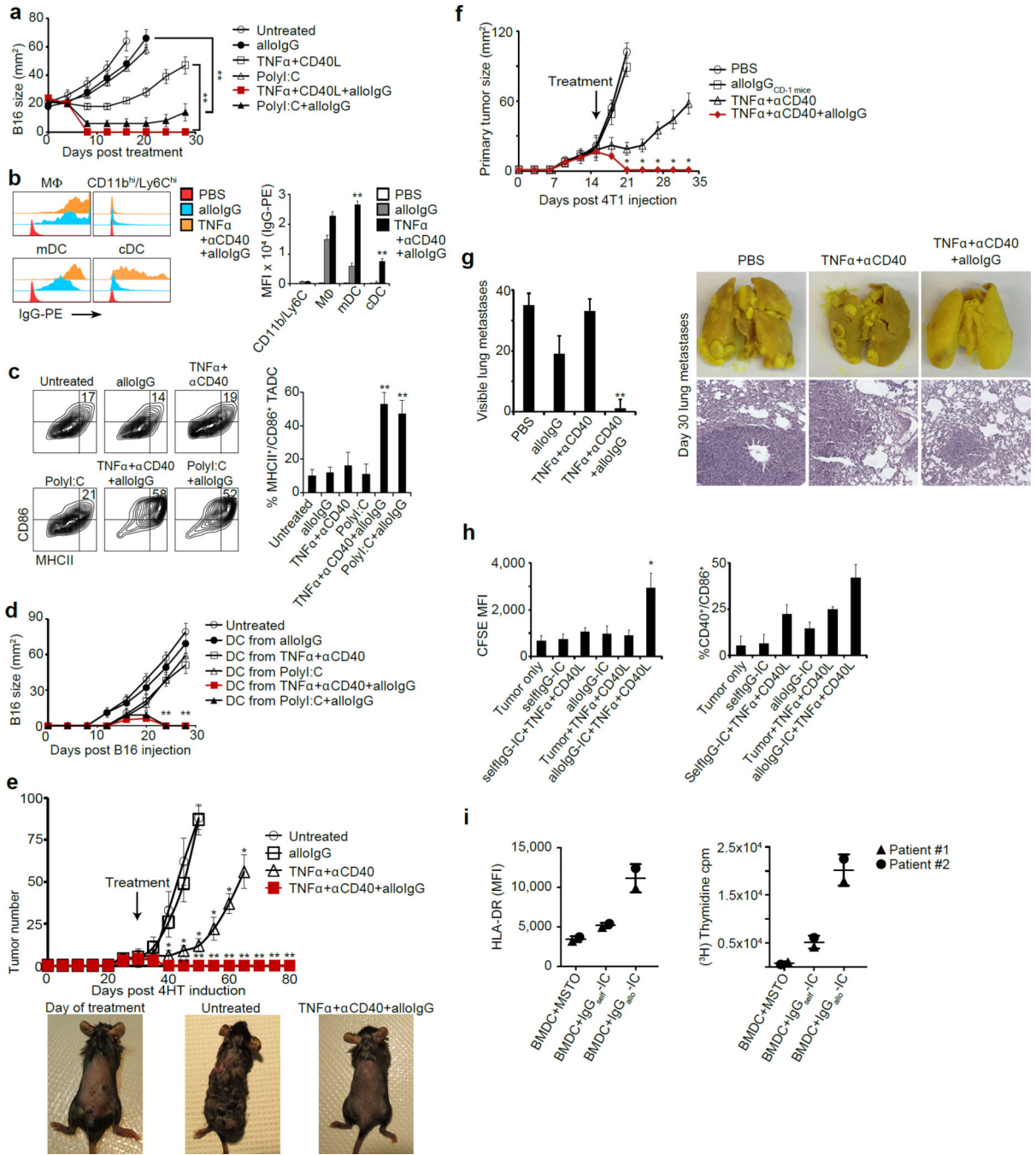


Figure 4. Injection of tumors *in situ* with alloantibodies in combination with CD40 agonists and TNF α induces systemic DC-mediated anti-tumor immunity

a. Growth of tumors injected with alloIgG, with or without immune stimuli (n=6). **b.** Mean fluorescence of PE in myeloid cells from B16-bearing mice 2h after treatment (n=4). **c.** CD86 and MHCII expression on DC from B16 tumors 5d following treatment (n=6). **d.** B16 growth in mice vaccinated with 2x10⁶ DC transferred from treated or untreated B16 tumors (n=6). **e.** Tumor number in Tyr:CreER;Braf^{V600E}/Pten^{lox/lox} mice following treatment (n=4). Photographs show representative mice on the day of treatment and after day 24. **f.** 4T1 tumor

size in mice following treatment (n=5). **g.** Mean counts of visible lung metastases, photographs and histology on day 30 (magnification: 10x, n=5). **h.** CFSE internalization and CD40/CD86 co-expression on TADC from lung cancer patients cultured overnight with CFSE-stained autologous tumor cells coated with selfIgG or alloIgG (n=2). **i.** HLA-DR upregulation by DC (left) and proliferative response of CD4⁺ T cells (right) from mesothelioma (MSTO) patients after culture of autologous BMDC with selfIgG- or alloIgG-coated autologous tumor cells (n=2). Mouse experiments were independently repeated at least 3 times and analyzed by Mann–Whitney U test. Asterisk (*) denotes p<0.05 and two asterisks (**) denote p<0.01.

Author Manuscript

Author Manuscript

Author Manuscript

Author Manuscript